OPEN ACCESS Freely available online

PLOS ONE

A Collection of Primary Tissue Cultures of Tumors from Vacuum Packed and Cooled Surgical Specimens: A Feasibility Study

Laura Annaratone[1☯], Caterina Marchiò[1,2☯], Rosalia Russo[1], Luigi Ciardo[1], Sandra Milena Rondon-Lagos[1], Margherita Goia[1], Maria Stella Scalzo[1,2], Stefania Bolla[1,2], Isabella Castellano[1,2], Ludovica Verdun di Cantogno[2], Gianni Bussolati[1,3], Anna Sapino[1,2]*

1 Department of Medical Sciences, University of Turin, Turin, Italy, **2** Department of Laboratory Medicine, Azienda Ospedaliera Città della Salute e della Scienza di Torino, Turin, Italy, **3** Institut Victor Babes, Bucharest, Romania

Abstract

Primary cultures represent an invaluable tool to set up functional experimental conditions; however, creation of tissue cultures from solid tumors is troublesome and often unproductive. Several features can affect the success rate of primary cultures, including technical issues from pre-analytical procedures employed in surgical theaters and pathology laboratories. We have recently introduced a new method of collection, transfer, and preservation of surgical specimens that requires immediate vacuum sealing of excised specimens at surgical theaters, followed by time-controlled transferring at 4°C to the pathology laboratory. Here we investigate the feasibility and performance of short-term primary cell cultures derived from vacuum packed and cooled (VPAC) preserved tissues. Tissue fragments were sampled from 52 surgical specimens of tumors larger than 2 cm for which surgical and VPAC times (the latter corresponding to cold ischemia time) were recorded. Cell viability was determined by trypan blue dye-exclusion assay and hematoxylin and eosin and immunohistochemical stainings were performed to appreciate morphological and immunophenotypical features of cultured cells. Cell viability showed a range of 84–100% in 44 out of 52 (85%) VPAC preserved tissues. Length of both surgical and VPAC times affected cell viability: the critical surgical time was set around 1 hour and 30 minutes, while cells preserved a good viability when kept for about 24 hours of vacuum at 4°C. Cells were maintained in culture for at least three passages. Immunocytochemistry confirmed the phenotype of distinct populations, that is, expression of cytokeratins in epithelioid cells and of vimentin in spindle cells. Our results suggest that VPAC preserved tissues may represent a reliable source for creation of primary cell cultures and that a careful monitoring of surgical and cold ischemia times fosters a good performance of primary tissue cultures.

Citation: Annaratone L, Marchiò C, Russo R, Ciardo L, Rondon-Lagos SM, et al. (2013) A Collection of Primary Tissue Cultures of Tumors from Vacuum Packed and Cooled Surgical Specimens: A Feasibility Study. PLoS ONE 8(9): e75193. doi:10.1371/journal.pone.0075193

Editor: Jorge Sans Burns, University Hospital of Modena and Reggio Emilia, Italy

Received March 27, 2013; **Accepted** August 13, 2013; **Published** September 30, 2013

Funding: This work was supported by Ricerca Sanitaria Finalizzata RF-2010-2310674 and AIRC Grants (IG 10787 to AS and MFAG 13310 to CM). GB is funded in part by Persother (SMIS-CSRN:549/12.024). The funders had no role in study design, data collection and analysis, decision to publish, or preparation of the manuscript.

Competing Interests: The authors have declared that no competing interests exist.

* E-mail: anna.sapino@unito.it

☯ These authors contributed equally to this work.

Introduction

Primary cultures represent an invaluable tool to set up functional experimental conditions that are instrumental to demonstrate biological mechanisms directly on human-derived tumor cells, however, creation of tissue cultures from solid tumors is troublesome and often unproductive particularly when dealing with primary cultures of carcinomas. Major biological issues are related to a relatively slow doubling time of epithelial cancer cells and to a rapid overgrowth with fibroblasts [1], depending also on the type of source lesions. In addition, technical aspects may affect the success rate of primary cultures in general. Such technical issues may stem from pre-analytical procedures routinely employed in surgical theaters and pathology laboratories. Indeed, two simple rules are mandatory for obtaining proper samples for cell cultures: (i) to acquire fresh specimens as soon as possible after completing the surgical procedure; (ii) to avoid both bacterial and fungal contamination of the specimens. The first rule matches with the need to reduce the ischemia process following the surgical procedure that stops with proper specimen fixation, since it allows activation of tissue enzymes, autolysis and degradation of proteins and nucleic acids [2,3]. However, logistics management of specimens from the surgical theater to the pathology lab has to be considered with the priority that involves material handling, packaging and transportation. Depending on the hospital structure the transport of surgical specimens from the surgical theater to the pathology lab may prolong the ischemia time. In addition, transfer may be performed using the most variable types of boxes, transport media and at different temperatures and the interval between surgical intervention and sampling at the pathology laboratory is not monitored. A good model for preserving sterility and cell viability could be that proposed for preserving organ for

transplantation, in which the first goal is reached by packing the organ in several layers of sterile containers and the second by cooling at 4°C the organ by surrounding it with an icy slush mixture [4]. In our University hospital we have recently introduced a new method of collection, transfer and preservation of surgical specimens [5,6,7,8]. This method requires immediate vacuum sealing of excised specimens at surgical theaters, followed by time-controlled transferring at 4°C to the pathology laboratory [6,7]. Such a procedure allows for having fresh (i.e. not fixed) tissues and it has been demonstrated not to affect morphology and to best preserve nucleic acids (DNA and RNA) and proteins [6,7,9].

In this study we tested the feasibility of setting up primary cell cultures derived from vacuum packed and cooled (VPAC) preserved tissues and to evaluate their performance and success rates.

Materials and Methods

Reagents

Tissue samples for cell cultures were collected in RPMI 1640 serum free medium, supplemented with 1% penicillin-streptomycin-fungizone.

The basal media used for cell culture was a mixture of DMEM (Dulbecco's Modified Eagle Medium) and F12 in 1:1 proportion. For preparation of complete media, 10% fetal bovine serum (FBS), 1% L-glutamine and 1% penicillin-streptomycin-fungizone were added to the basal media mixture. The complete media was supplemented with 10 ng/mL human epidermal growth factor (EGF), 5 μg/mL insulin and 400 ng/mL hydrocortisone. For breast cancer samples, the complete media contained also 5 ng/mL 17-beta-estradiol and 500 ng/mL progesterone.

For enzymatic cell dissociation Collagenase Type IV was used while trypsin-EDTA was used for passaging. All reagents were from Sigma-Aldrich, St Louis, MO, USA.

All materials used in this experiment were sterile to prevent contamination.

Vacuum Sample Collection

The study was approved by the ethic institutional review board for "Biobanking and use of human tissue for experimental studies" of the Pathology Services of the Azienda Ospedaliera Città della Salute e della Scienza di Torino. Written informed consent was obtained from all patients for their tissue to be used in research. Following excision in the surgical theater, surgical specimens were immediately placed into beta-ray sterilized plastic bags and vacuum sealed using the TissueSAFE machine (Mod. VAC 10, by Milestone, Bergamo, Italy; see www.milestonemedsrl.com), according to a procedure originally reported by our group [7] and currently implemented as a standard technique in our hospital [5,8]. The VPAC specimens were kept and transferred to the pathology lab at 4°C in a chilled plastic box. Once in the lab, tissues were kept in a refrigerator at 4°C until processing. The surgical and VPAC times of the sample and the histotype, the percentage of stroma and epithelial cells of sample received from surgical theaters were recorded in a dedicated database.

As a separate analysis, two large specimens of reduction mammoplasty were divided in three parts (each of approximately 10×5×5 cm) in order to evaluate the decrease of temperature by using a digital thermometer with stainless steel sensor probe at different conditions of storage (i.e. vacuum sealed at room temperature, vacuum sealed at 4°C, not vacuum sealed at 4°C).

Cell Culture Procedure

The study was conducted on surgical specimens of tumors larger than 2 cm, leading to a cohort of 52 surgical samples, including 13 colorectal carcinomas, 6 lung carcinomas, 27 breast carcinomas, 2 adrenocortical adenomas, 3 gastric carcinomas and 1 thyroid carcinoma (see Table 1 for details). Samples for cell cultures were collected from "left over tissues" (i.e. tissue residuals not used for diagnostic and therapeutic purposes) by using sterile scalpels. Samples of 1×1 cm around 0.5 cm in thickness were collected in sterile tubes containing 10 mL of RPMI serum free medium, supplemented with 1% penicillin-streptomycin-fungizone. Tissue samples were washed 3 times in 20 mL of the same medium, then finely minced by surgical blades into approximately 1×1 mm fragments and divided in two aliquots. One aliquot was processed for cryopreservation, while the other tissue fragments were incubated at 37°C with collagenase type IV (1 mg/mL; 1:1 RPMI, final volume 10 mL), for 3–5 hours until complete disaggregation of fragments was obtained. Digested samples were shaken vigorously by hand to disaggregate possible residual large clumps. Collagenase activity was blocked by addition of 10 mL of RPMI with 10% FBS. After centrifugation at 800 rcf for 6 minutes, the cell pellets were re-suspended in complete culture medium. The final cell suspension was seeded in Petri dishes as passage 0 and kept in a humidified incubator with 5% CO_2 at 37°C. Culture medium was changed first at the time of cell attachment and, subsequently, three times a week. Cell growth was monitored daily in flasks with an EVOS inverted microscope (Advanced Microscopy Group, Bothell, WA, USA) during the first week. The morphology of the cell population (spindle or mixed spindle-epithelioid) was recorded.

Whenever the cell pellet was adequate, cells were seeded in another Petri dish containing sterilized coverslips (22×22 mm) to carry out Hematoxylin and Eosin (H&E) staining and immunocytochemical (ICC) reactions. Each time cells grown at confluence were split was considered a new passage.

Viability Assay and Cryopreservation of Cells

Viability of cells was determined by trypan blue dye (0.4% in PBS)-exclusion assay. Aliquots of cell suspension were incubated with trypan blue solution (1:1) for 5 min. Finally cells were transferred to the Burker chamber and counted by light microscope. Dead cells were defined as those stained with the dye. The percentage of living cells was calculated by the relationship between the number of viable cells and the total number of cells counted. Aliquots of cells were cryopreserved into sterile cryo-tubes in 1.5 mL freezing medium (FBS containing 10% DMSO). Tubes were kept at −80°C (for a maximum of 6 weeks) or, following overnight cooling, transferred into liquid nitrogen (for longer storage periods).

H&E Staining and ICC Reactions

To evaluate the proportion of stroma and tumor cells in the sample collected for primary cultures we examined the H&E histological slide obtained from sampling of a parallel tumor area. To evaluate morphology of cultures, cells were grown on coverslips (sealed on a standard slide) and washed in phosphate-buffered saline (PBS 1X) for 5 minutes, fixed in 4% neutral-buffered formalin for 10 minutes and dehydrated through a series of alcohols up to absolute alcohol and stained with H&E staining.

If the culture showed a mixed population we tried to characterize the cells using specific organ related markers. ICC was performed using an automated slide processing platform (Ventana BenchMark XT AutoStainer, Ventana Medical Systems, Tucson, AZ, USA). The following primary antibodies were used:

Table 1. Details of the 52 source lesions for cell cultures included in the study, correspondent surgical, and VPAC times of the specimens and percentage of viable cells in the primary cultures.

				Tumor histology			Cell culture	
#	Organ	Surgical Time [hours (h), minutes (′)]	VPAC Time [hours (h), minutes (′)]	Histological Type	% Stroma	% Tumor Cells	% Cell Viability	Cell Population
1	Colon	1h45′	3h45′	ADC	30	70	**0.0%**	/
2	Stomach	2h15′	4h10′	ADC	20	80	**0.0%**	/
3	Lung	1h20′	4h15′	ADC	40	60	**95.3%**	Spindle
4	Lung	1h20′	4h30′	ADC	40	60	**93,9%**	Mixed
5	Stomach	1h30′	4h45′	ADC	35	65	**97,0%**	Spindle
6	Colon	1h10′	5h00′	ADC	15	85	**100,0%**	Mixed
7	Colon	0h40′	5h25′	ADC	5	95	**96,8%**	Mixed
8	Colon	1h15′	5h25′	ADC	30	70	**92,2%**	Mixed
9	Adrenal	1h20′	5h25′	ADENOMA	10	90	**86,1%**	Spindle
10	Breast	1h35′	20h40′	ILC	40	60	**0,0%**	/
11	Lung	2h15′	21h20′	SFT	8	92	**96,4%**	Mixed
12	Breast	0h45′	21h40′	IC-NST	25	75	**93,6%**	Mixed
13	Breast	1h40′	21h43′	IC-NST	10	90	**94,8%**	Mixed
14	Breast	0h20′	22h20′	ILC	8	92	**98,8%**	Mixed
15	Breast	0h55′	22h20′	IC-NST	15	85	**95,0%**	Mixed
16	Colon	1h10′	22h30′	ADC	30	70	**92,2%**	Spindle
17	Lung	0h10′	22h35′	ADC	2	98	**97,7%**	Mixed
18	Lung	1h20′	22h35′	SC	50	50	**96,5%**	Mixed
19	Colon	1h20′	22h45′	ADC	40	60	**93,5%**	Spindle
20	Breast	1h10′	23h10′	IC-NST	20	80	**96,9%**	Mixed
21	Breast	0h11′	23h17′	IC-NST	50	50	**96,6%**	Mixed
22	Breast	1h50′	23h20′	IC-NST	60	40	**96,3%**	Mixed
23	Breast	0h25′	23h25′	ILC	50	50	**96,1%**	Mixed
24	Breast	1h10′	23h46′	IC-NST	40	60	**98,5%**	Mixed
25	Breast	0h05′	23h50′	IC-NST	30	70	**95,9%**	Mixed
26	Colon	0h45′	23h50′	ADC	15	85	**86,6%**	Mixed
27	Breast	1h10′	23h50′	MC	10	90	**94,0%**	Mixed
28	Breast	1h20′	24h00′	IC-NST	55	45	**84,0%**	Spindle
29	Breast	0h50′	24h10′	IC-NST	30	70	**97,9%**	Mixed
30	Breast	0h25′	24h16′	IC-NST	10	90	**99,3%**	Mixed
31	Breast	0h15′	24h30′	IC-NST	20	80	**99,2%**	Mixed
32	Breast	1h10′	24h35′	IC-NST	65	35	**0,0%**	/
33	Breast	0h40′	25h00′	PDC	30	70	**96,5%**	Mixed
34	Lung	1h40′	25h00′	ADC	40	60	**97,3%**	Spindle
35	Breast	0h50′	25h05′	ILC	40	60	**96,7%**	Mixed
36	Breast	0h35′	25h20′	IC-NST	30	70	**96,0%**	Mixed
37	Colon	1h45′	26h10′	ADC	40	60	**98,6%**	Spindle
38	Thyroid	2h20′	26h40′	HCC	20	80	**96,3%**	Mixed
39	Colon	1h45′	27h40′	ADC	25	75	**90,7%**	Spindle
40	Breast	0h27′	28h20′	ILC	30	70	**0,0%**	/
41	Colon	0h50′	29h00′	ADC	20	80	**86,5%**	Mixed
42	Colon	1h25′	39h20′	ADC	20	80	**0,0%**	/
43	Breast	0h50′	42h15′	IC-NST	40	60	**89,0%**	Mixed
44	Breast	0h20′	43h05′	ILC+IPC	25	75	**97,3%**	Mixed
45	Breast	1h00′	45h05′	IC-NST	80	20	**98,9%**	Spindle

Table 1. Cont.

				Tumor histology			Cell culture	
#	Organ	Surgical Time [hours (h), minutes (′)]	VPAC Time [hours (h), minutes (′)]	Histological Type	% Stroma	% Tumor Cells	% Cell Viability	Cell Population
46	Breast	3h00′	45h50′	IC-NST	40	60	**98,7%**	Mixed
47	Breast	0h40′	46h47′	IC-NST	20	80	**96,3%**	Mixed
48	Colon	1h10′	70h15′	ADC	30	70	**97,5%**	Spindle
49	Breast	2h25′	72h25′	ILC	20	80	**95,5%**	Mixed
50	Colon	1h45′	73h45′	ADC	25	75	**96,7%**	Spindle
51	Adrenal	3h45′	74h05′	PHEO	5	95	**0,0%**	/
52	Stomach	1h30′	75h15′	ADC	52	48	**0,0%**	/

Legend: ADC: adenocarcinoma; HCC: Hurtle cell carcinoma; IC-NST: invasive carcinoma of no special type; ILC: infiltrating lobular carcinoma; IPC: intracystic papillary carcinoma; MC: medullary carcinoma; PDC: poorly differentiated carcinoma; PHEO: pheochromocytoma; SFT: solitary fibrous tumor; SC: squamous carcinoma.
doi:10.1371/journal.pone.0075193.t001

mouse anti-pancytokeratin (clone AE1-AE3-PCK26, Ventana; pre-diluted, antigen retrieval: Protease 1 (Ventana) for 4 minutes), anti-vimentin (clone R9, Dako, Glostrup, Denmark; dilution 1:50, antigen retrieval: pre-diluted pretreatment solution Cell Conditioning 1 (CC1, Ventana) for 20 minutes), anticytokeratin-19 (clone NCL-CK19, Leica Novocastra; dilution 1:50, antigen retrieval: CC1 36 for minutes), anti-cytokeratin-14 (clone NCL-LL002, Leica Novocastra; dilution 1:100, antigen retrieval: CC1 for 36 minutes), anti-cytokeratin-7 (clone OVTL, Dako, Glostrup, Denmark; dilution 1:100, antigen retrieval: CC1 for 36 minutes) and anti-TTF1 (clone 8G7G3/1, Roche Diagnostics; pre-diluted, antigen retrieval: CC1 for 36 minutes).

Statistical Analysis

Results were analyzed by contingency tables using the Fisher's exact test. Paired Student's T-test was used for continuous variables. A p value <0.05 was considered statistically significant.

Results

Effect of Vacuum and Cooling on Specimen Temperature

VPAC produced a more rapid decrease of temperature as compared to non-VPAC procedures, while vacuum sealing at room temperature did not significantly affect temperature decrease (Figure 1). Statistically significant differences between groups were observed at 1 hour and 2 hours ($p = 0.005$ and $p = 0.013$, respectively). The results were consistent for the whole set of samples obtained from two different reduction mammoplasty specimens.

Cell Viability and Influence of Surgical and VPAC Time

Table 1 lists the details of 52 collected cases (site of lesion origin, histotype and percentage of stromal and tumor components) with correspondent surgical time (i.e. the time between the beginning of surgery - incision of the skin - and the surgical removal of tissues) and VPAC time (i.e. time between surgical removal of tissues and

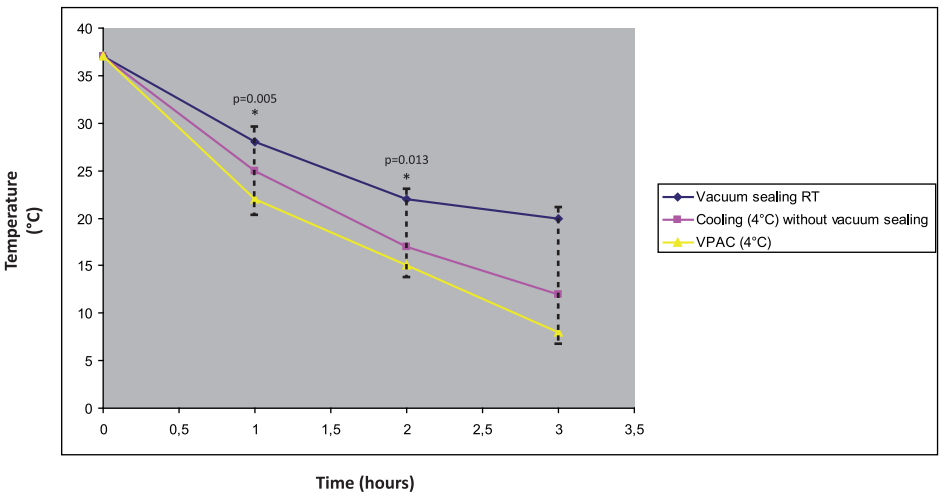

Figure 1. Effect of vacuum and cooling on specimen temperature. Results of temperature monitoring over time of a specimen of reduction mammoplasty. The specimen was subdivided in three parts that were stored under three distinct conditions, i.e. vacuum sealed at room temperature (RT), vacuum sealed at 4°C, cooled at 4°C without vacuum sealing. VPAC produced a more rapid decrease of temperature than non-VPAC procedures, while vacuum sealing at room temperature did not significantly affect temperature decrease. The * indicates statistically significant differences ($p = 0.005$ at 1 hour, $p = 0.013$ at 2 hours).
doi:10.1371/journal.pone.0075193.g001

A

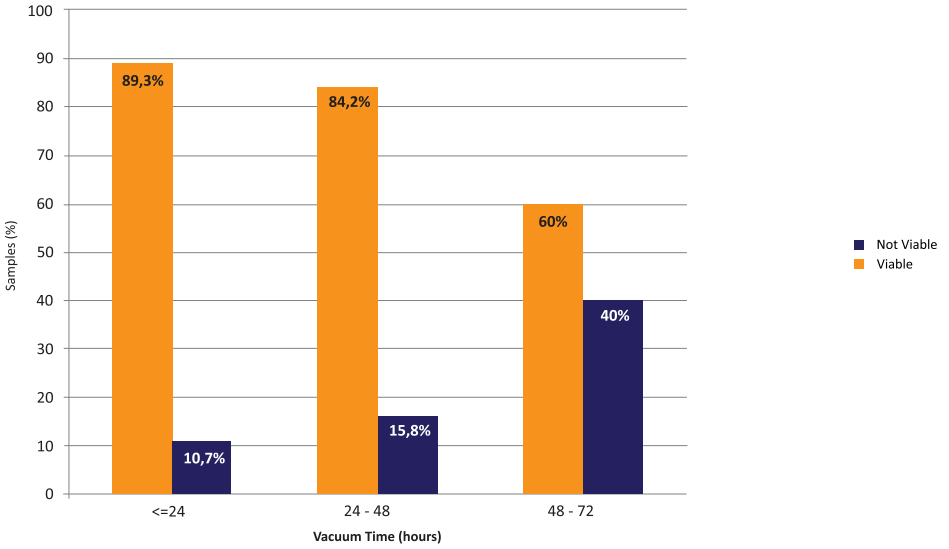
100
90
80
70
60
50
40
30
20
10
0
Samples (%)
89,3%
10,7%
84,2%
15,8%
60%
40%
<=24
24 - 48
48 - 72
Vacuum Time (hours)
Not Viable
Viable

B

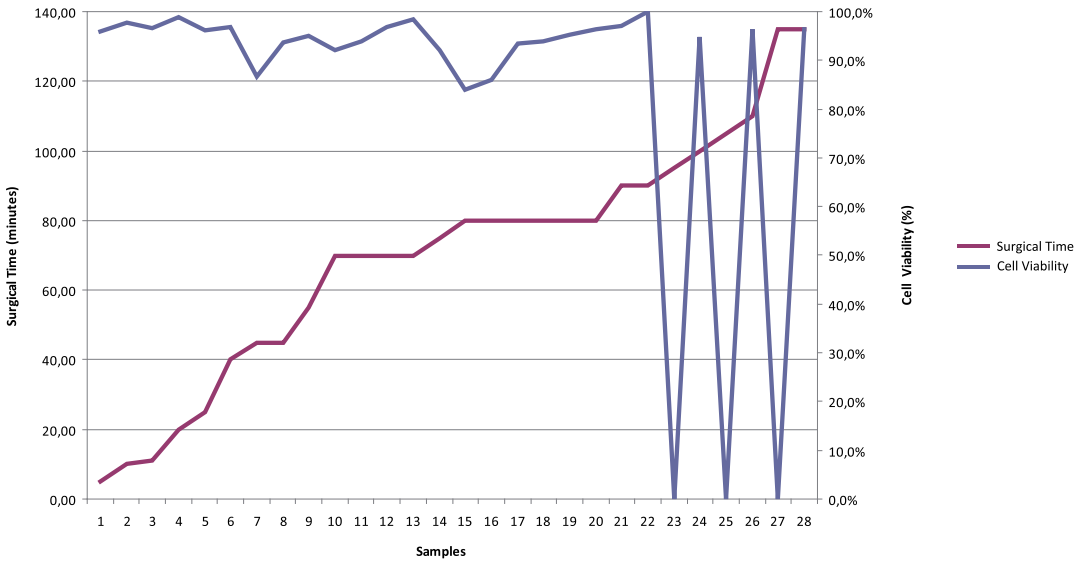
140,00
120,00
100,00
80,00
60,00
40,00
20,00
0,00
Surgical Time (minutes)
100,0%
90,0%
80,0%
70,0%
60,0%
50,0%
40,0%
30,0%
20,0%
10,0%
0,0%
Cell Viability (%)
1 2 3 4 5 6 7 8 9 10 11 12 13 14 15 16 17 18 19 20 21 22 23 24 25 26 27 28
Samples
Surgical Time
Cell Viability

C

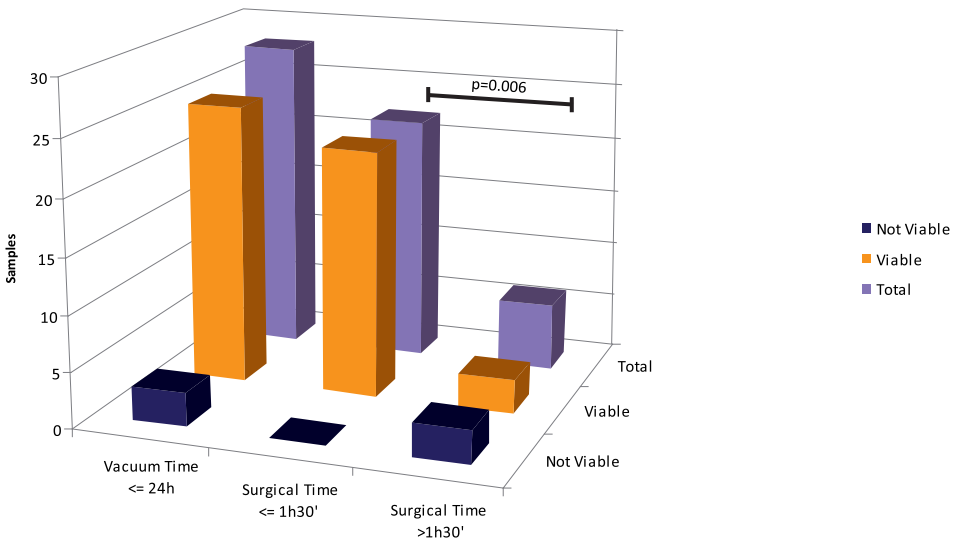
30
25
20
15
10
5
0
Samples
p=0.006
Total
Viable
Not Viable
Vacuum Time
<= 24h
Surgical Time
<= 1h30'
Surgical Time
>1h30'
Not Viable
Viable
Total

Figure 2. Reciprocal relationship between surgical and VPAC times with cell viability. A: cell viability was 89.3% in specimens with VPAC ≤24 h, 84.2% in specimens with 24 h<VPAC≤48 h and 60% in specimens with VPAC >48 h. B: The critical surgical time was set around 1 hour and 30 minutes, as shown by the drop of cell viability line as compared to the surgical time. This analysis was performed in the subset of specimens with VPAC time ≤24 h (in order not to introduce a bias due to long cold ischemia time). C: Assessment of cell viability in specimens with VPAC time ≤24 h and comparison with surgical time. The histogram shows the number of viable and not viable cell cultures obtained from samples with a VPAC time ≤24 h: total number of specimens with VPAC time ≤24 h on the left, specimens with VPAC time ≤24 h and surgical time ≤1 hour and 30 minutes in the middle, specimens with VPAC time ≤24 h and surgical time >1 hour and 30 minutes on the right. The difference in cell viability between the two groups (surgical time <1 hour and 30 minutes and surgical time >1 hour and 30 minutes) was statistically significant (p = 0.006, Fisher's exact test).
doi:10.1371/journal.pone.0075193.g002

their fixation, i.e. "cold ischemia time"). Both surgical and VPAC times were highly variable (Table 1). For 28 cases the VPAC time was 0< hours ≤24, for 19 cases it was 24< hours ≤48, for 2 cases it was 48< hours <72, for 3 cases it was >72 hours. Establishment of short-term primary cultures was successfully achieved in 85% of processed samples (44 out of 52), regardless of the specimen size and origin and cellularity of source lesions. Only one case of gastric cancer developed bacterial infection after one day of culture (Table 1, case #2). Cell viability ranged from 84 to 100% (mean: 95.2%) in the 44 obtained primary cultures. Length of both surgical and VPAC times affected cell viability. Cells preserved a good viability when kept for about 24–48 hours of VPAC at 4°C (Figure 2A), while the critical surgical time was set around 1 hour and 30 minutes (Figure 2B). More specifically, the cut-off time of 1 hour and 30 minutes for surgical time was data-driven as follows: first, we focused on 27 samples with VPAC time ≤24 h, in order not to introduce a bias due to a long cold ischemia time. Within such a subgroup we found that with the increased surgical times cell viability was maintained (≥84%) up to the cut-off time of 1 hour and 30 minutes (Figure 2B). Beyond that period, cell viability

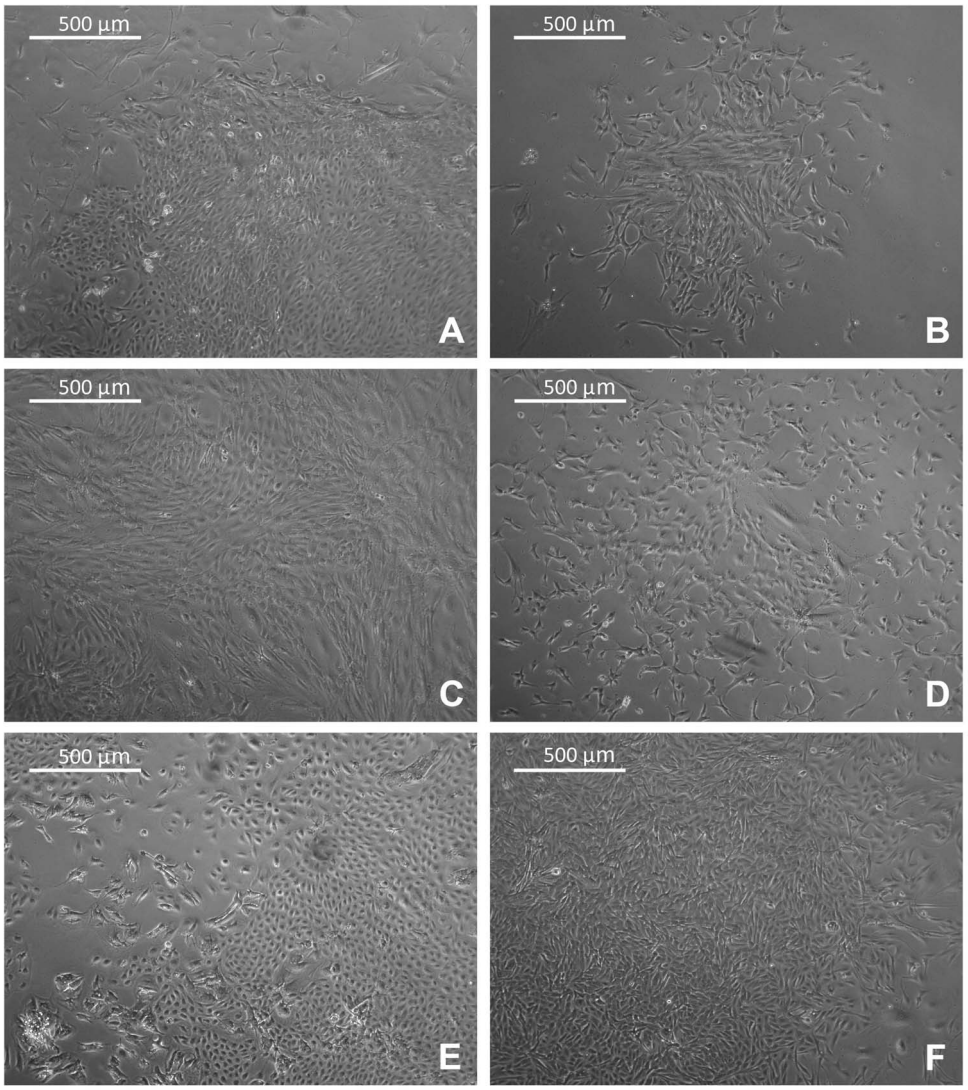

Figure 3. Primary cell cultures in flasks. EVOS inverted microscope images (4× magnification) of primary cell cultures of tumors from different organs growing adhering to the flasks. A: breast carcinoma; B: colorectal carcinoma; C: lung adenocarcinoma; D: gastric carcinoma; E: pheochromocytoma; F: Hurtle cell carcinoma of the thyroid.
doi:10.1371/journal.pone.0075193.g003

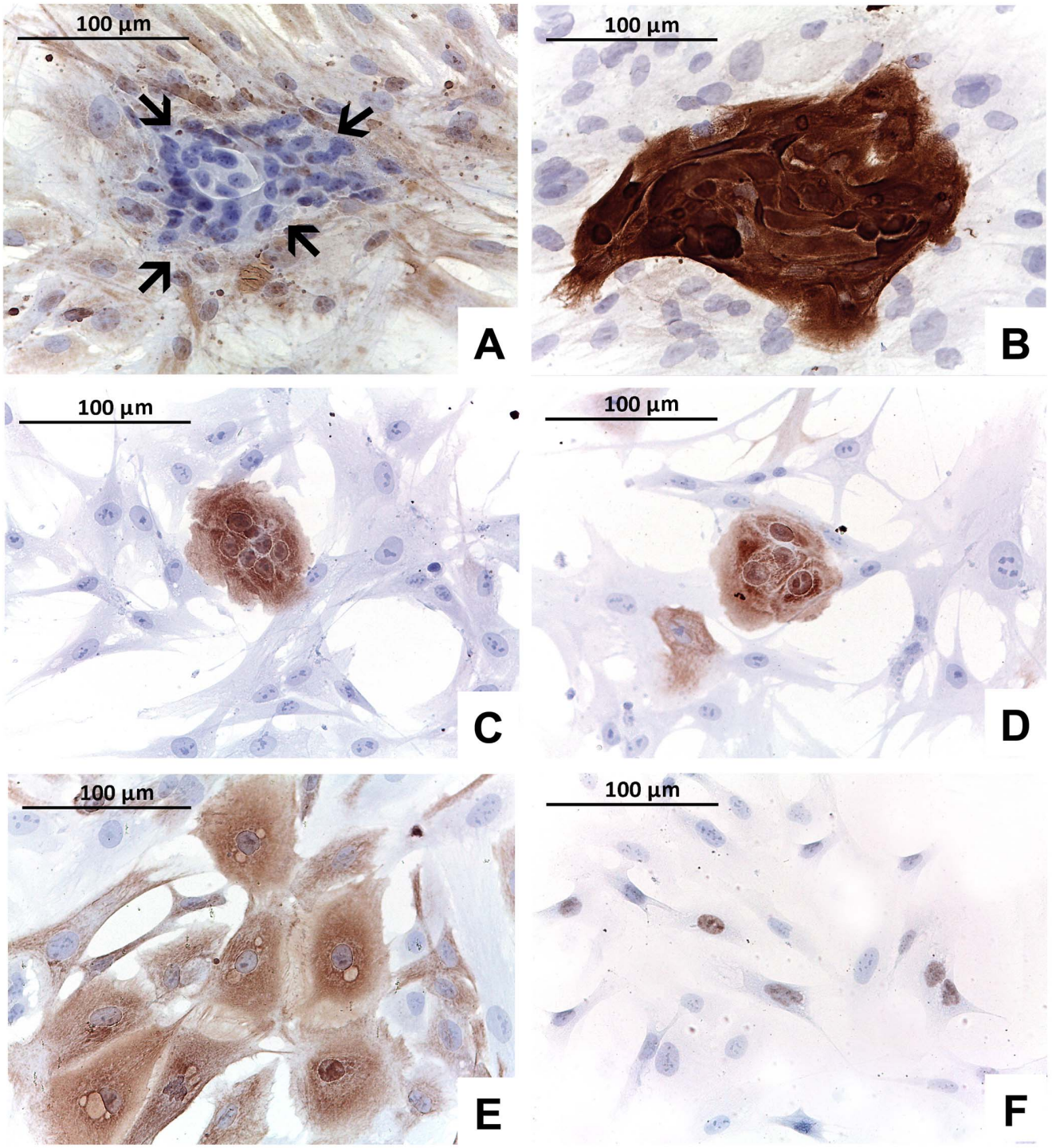

Figure 4. Immunophenotype of cells. A, B: primary culture from an invasive carcinoma of no special type of the breast composed of a mixed population: fibroblasts positive for vimentin (A; arrows indicate epithelial cells) and epithelial cells showing strong cytokeratin-19 positivity (B). C, D: primary culture raised from a lung adenocarcinoma shows epithelial cells positive for cytokeratin-19 (A) and cytokeratin-7 (B). E, F: cells from a primary culture of a Hurtle cell carcinoma of the thyroid show positivity for cytokeratin-19 (E) and TTF1 (F).
doi:10.1371/journal.pone.0075193.g004

dropped to 0% in 3/6 cases, two of which had VPAC time shorter than 5 hours (Table 1 case #1 and #2). The difference in cell viability between the two groups (surgical time <1 hour and 30 minutes and surgical time >1 hour and 30 minutes) was statistically significant ($p = 0.006$, Fisher's exact test) (Figure 2B).

Then, we analyzed the influence of VPAC time on cell viability in more in details. Cell growth was not feasible in 10.7% of specimens with VPAC time ≤24 hours, in 15.8% of tissues with 24< hours ≤48 VPAC time and in 40% of samples with >48 hours VPAC time (no statistically significant differences between the groups) (Figure 2A). However, the examination of the

corresponding histological samples showed preservation of morphology regardless of surgical and VPAC times.

Characterization of Cell Primary Cultures

The relative percentage of stroma *versus* tumor, as derived from histological slides, seemed not to affect the morphology of cell cultures. In 12 out of 44 viable cultures (27%) the cell population had uniform spindle morphology since the first passage (Table 1). Mixed cell population of spindle and epithelioid cells (Table 1, Figure 3, Figure 4) was observed in the remaining 32 (73%) primary cultures. In cultures derived from adenocarcinomas of breast, lung and colon the epitheliod islets were clearly observed within the spindle components (Figure 4). In 12 out of 32 (37.5%) cases the mixed population could be maintained in culture for three passages. However, in the remaining 20 cases (62.5%) spindle cells that exhibited a great propensity to proliferate *in vitro* overgrew epithelioid cells soon after the first passages (Figure 3). The spindle cell overgrowth was variable across the samples and occurred between passage 2 and passage 5. The results of ICC, performed in primary cultures at first passage, confirmed the phenotype of distinct populations (Figure 4). The mutual exclusive expression of cytokeratins in epithelioid cells and of vimentin in spindle cells suggested the epithelial and stromal nature of cultured cells, respectively (Figure 4). A word of caution for the vimentin positivity in cell cultures should be considered because it is not uncommon to observe vimentin expression in cell cultures of epithelial origin [10,11,12]. However in our hand none of the epithelial like cells expressed vimentin, at least at the first passages. Epithelial cells were further characterized by highlighting positivity for tissue-specific cytokeratins, such as cytokeratin-19 for breast and thyroid carcinomas and cytokeratin 7 for lung carcinomas (Figure 4). Cytokeratin-14, studied in breast samples, was expressed neither in the tumor of origin nor in the related cell cultures. TTF1 was instead expressed in thyroid carcinoma and lung adenocarcinomas (Figure 4).

Discussion

In this feasibility study we report on the setting up of primary cultures from VPAC surgical specimens. By sampling tissue fragments from VPAC preserved specimens we achieved a success rate of approximately 85% leading to a collection of short-term tissue cultures from different neoplastic lesions.

Since the adoption at our institution of an innovative method for tissue collection, transport and storage of surgical specimens based on VPAC technology [5,7,8], we have demonstrated in these specimens optimal tissue morphology as well as integrity of antigens for ICC and excellent preservation of nucleic acids to perform molecular analyses [6,9]. We now show a further implementation of VPAC technology.

The establishment of primary cultures of tumor cells is the goal of many laboratories, however the technique is troublesome, time consuming with a very variable performance rate [1,13].

When approaching the creation of cell cultures from fresh tumor lesions, collaboration with the pathology laboratory is mandatory. Although the multi-step process involving the creation of a primary culture should stem from a proper tissue handling and sampling, the impact of pre-analytical variables is usually disregarded. In particular, we showed that the surgical time can influence cell viability. In organ transplantation the surgical time may have different definitions and it remains a topic of debate [14,15,16]. For cell culture the surgical time starts from the vessel clamping during surgical procedure (corresponding to the loss of perfusion or oxygenation) and ends with the organ excision. It has been shown that significant transcript alterations occur simply as a result of surgical excision [17]. To our knowledge this is the first study that evaluates the effect of the time of surgery on cell viability. We established that the optimal time should be within 1 hour and 30 minutes from the starting of the surgical procedure. During this time the tissue remains alive and is reactive. The temperature of the specimens during surgery decreases very slowly, however disruption of blood flow leads to progressive tissue ischemia and hypoxigenation that cause alterations of cell membrane and receptors, ion regulation, and enzyme systems [18,19].

The cold ischemia time (which in our study corresponds to the VPAC time) starts when the specimen is excised and ends with incision of tissue and placement in a suitable tissue fixative [18,19]. Appreciation of the scientific importance of primary tissue handling procedures is growing, particularly for its impact on preservation of nucleic acids and proteins [20,21,22,23,24]. When dealing with cell cultures and xenograft implantations researchers may ideally wish to collect the sample for experiments directly in the surgery room in order to keep the cold ischemia time as short as possible. However, any such sampling may lead to problems for pathologists in terms of correct gross evaluation of tumor samples (status of surgical margins, staging etc.).

Another issue that should be considered is the optimal temperature to guarantee cell viability. In transplantation pathology it has been shown that a rapid induction of hypothermia at 0–4°C by perfusion of organ with specific solutions better preserves organ viability [25,26]. We have proposed transfer of surgical specimens vacuum-sealed using a chilled plastic box at 4°C [6,7]. Our results suggest the avoidance of insulating air around tissues with the VPAC system allows faster cooling at 4°C. From our experience on nucleic acid preservation [7,9] it seems that it is the prompt cooling that principally influences preservation. This has also been confirmed by independent observations [27] that show that storage at 4°C preserved tissues to a higher degree than storage at room temperature, independently of whether the tissue was subjected to vacuum sealing or not. With this study we prove that VPAC maintains cell viability even after 70 hours, however, as expected, for longer VPAC times, the percentage of cell death increased. Finally, the vacuum sealing in beta-sterilized bags helped prevent bacterial and fungal contamination and consequently, we experienced cell culture infections in only 2% of specimens.

In conclusion, VPAC represented a reliable and reproducible tissue handling protocol for creation of primary cell cultures. Our results also showed how a careful monitoring of surgical and cold ischemia times fostered a good performance of primary tissue cultures. Further studies are needed to more carefully define key parameters governing the reliability of the VPAC method. Nonetheless, the environmentally safe VPAC collection, preservation and storage of surgical specimens already represented a helpful strategy to bridge diagnostic and experimental pathology, offering a new tool for biobanking and improved generation of primary cultures as clinically relevant models of neoplastic lesions.

Acknowledgments

We thank the personnel of the surgical theaters of the Breast Unit at our Institution (Azienda Ospedaliera Città della Salute e della Scienza di Torino) for the fruitful collaboration in setting up and working with the VPAC system.

Author Contributions

Conceived and designed the experiments: AS. Performed the experiments: LA CM RR LC SMRL MSS SB. Analyzed the data: LA CM MG LVdC IC GB AS. Contributed reagents/materials/analysis tools: CM AS. Wrote the paper: AS CM LA.

References

1. Speirs V (2004) Primary culture of human mammary tumor cells. In: Pfragner R, Freshney RI, editors. Culture of human tumor cells. Wilmington, DE: Wiley-Liss. Pp. 205–219.
2. Chung JY, Braunschweig T, Williams R, Guerrero N, Hoffmann KM, et al. (2008) Factors in tissue handling and processing that impact RNA obtained from formalin-fixed, paraffin-embedded tissue. J Histochem Cytochem 56: 1033–1042.
3. Medeiros F, Rigl CT, Anderson GG, Becker SH, Halling KC (2007) Tissue handling for genome-wide expression analysis: a review of the issues, evidence, and opportunities. Arch Pathol Lab Med 131: 1805–1816.
4. Mukherjee S (2011) Organ Preservation. In: Reference M, editor. Drugs, Diseases & Procedures.
5. Berton F, Novi CD (2012) Occupational hazards of hospital personnel: assessment of a safe alternative to formaldehyde. J Occup Health 54: 74–78.
6. Bussolati G, Annaratone L, Medico E, D'Armento G, Sapino A (2011) Formalin fixation at low temperature better preserves nucleic acid integrity. PLoS One 6: e21043.
7. Bussolati G, Chiusa L, Cimino A, D'Armento G (2008) Tissue transfer to pathology labs: under vacuum is the safe alternative to formalin. Virchows Arch 452: 229–231.
8. Di Novi C, Minniti D, Barbaro S, Zampirolo MG, Cimino A, et al. (2010) Vacuum-based preservation of surgical specimens: an environmentally-safe step towards a formalin-free hospital. Sci Total Environ 408: 3092–3095.
9. Comanescu M, Annaratone L, D'Armento G, Cardos G, Sapino A, et al. (2012) Critical steps in tissue processing in histopathology. Recent Pat DNA Gene Seq 6: 22–32.
10. Dairkee SH, Blayney CM, Asarnow DM, Smith HS, Hackett AJ (1985) Early expression of vimentin in human mammary cultures. In Vitro Cell Dev Biol 21: 321–327.
11. Pieper FR, Van de Klundert FA, Raats JM, Henderik JB, Schaart G, et al. (1992) Regulation of vimentin expression in cultured epithelial cells. Eur J Biochem 210: 509–519.
12. Thepot A, Desanlis A, Venet E, Thivillier L, Justin V, et al. (2011) Assessment of transformed properties in vitro and of tumorigenicity in vivo in primary keratinocytes cultured for epidermal sheet transplantation. J Skin Cancer 2011: 936546.
13. Wang CS, Goulet F, Lavoie J, Drouin R, Auger F, et al. (2000) Establishment and characterization of a new cell line derived from a human primary breast carcinoma. Cancer Genet Cytogenet 120: 58–72.
14. Piazza O (2013) Maximum tolerable warm ischaemia time in transplantation from non-heart-beating-donors. Trends in Anaesthesia and Critical Care 3(2): 72–76.
15. Bernat JL, D'Alessandro AM, Port FK, Bleck TP, Heard SO, et al. (2006) Report of a National Conference on Donation after cardiac death. Am J Transplant 6: 281–291.
16. Halazun KJ, Al-Mukhtar A, Aldouri A, Willis S, Ahmad N (2007) Warm ischemia in transplantation: search for a consensus definition. Transplant Proc 39: 1329–1331.
17. Lin DW, Coleman IM, Hawley S, Huang CY, Dumpit R, et al. (2006) Influence of surgical manipulation on prostate gene expression: implications for molecular correlates of treatment effects and disease prognosis. J Clin Oncol 24: 3763–3770.
18. Hicks DG, Kushner L, McCarthy K (2011) Breast cancer predictive factor testing: the challenges and importance of standardizing tissue handling. J Natl Cancer Inst Monogr 2011: 43–45.
19. Hicks DG, Kushner L, McCarthy K (2012) Breast cancer predictive factor testing: the challenges and importance of standardizing tissue handling. J Natl Cancer Inst Monogr 2011: 43–45.
20. Neumeister VM, Anagnostou V, Siddiqui S, England AM, Zarrella ER, et al. (2012) Quantitative assessment of effect of preanalytic cold ischemic time on protein expression in breast cancer tissues. J Natl Cancer Inst 104: 1815–1824.
21. Pekmezci M, Szpaderska A, Osipo C, Ersahin C (2012) The Effect of Cold Ischemia Time and/or Formalin Fixation on Estrogen Receptor, Progesterone Receptor, and Human Epidermal Growth Factor Receptor-2 Results in Breast Carcinoma. Patholog Res Int: 947041.
22. Portier BP, Wang Z, Downs-Kelly E, Rowe JJ, Patil D, et al. (2013) Delay to formalin fixation 'cold ischemia time': effect on ERBB2 detection by in-situ hybridization and immunohistochemistry. Mod Pathol 26: 1–9.
23. Yildiz-Aktas IZ, Dabbs DJ, Bhargava R (2012) The effect of cold ischemic time on the immunohistochemical evaluation of estrogen receptor, progesterone receptor, and HER2 expression in invasive breast carcinoma. Mod Pathol 25: 1098–1105.
24. Yildiz-Aktas IZ, Dabbs DJ, Cooper KL, Chivukula M, McManus K, et al. (2012) The effect of 96-hour formalin fixation on the immunohistochemical evaluation of estrogen receptor, progesterone receptor, and HER2 expression in invasive breast carcinoma. Am J Clin Pathol 137: 691–698.
25. Belzer FO, Southard JH (1988) Principles of solid-organ preservation by cold storage. Transplantation 45: 673–676.
26. D'Alessandro AM, Southard JH (2002) Hypothermic perfusion of the warm ischemic kidney: is 32 degrees C better than 4 degrees C? Am J Transplant 2: 689; author reply 690.
27. Kristensen T, Engvad B, Nielsen O, Pless T, Walter S, et al. (2011) Vacuum sealing and cooling as methods to preserve surgical specimens. Appl Immunohistochem Mol Morphol 19: 460–469.

MOLECULAR CYTOGENETICS

RESEARCH Open Access

Differences and homologies of chromosomal alterations within and between breast cancer cell lines: a clustering analysis

Milena Rondón-Lagos[1,3], Ludovica Verdun Di Cantogno[2], Caterina Marchiò[1,2], Nelson Rangel[1], Cesar Payan-Gomez[3,4], Patrizia Gugliotta[1], Cristina Botta[1], Gianni Bussolati[1], Sandra R Ramírez-Clavijo[3], Barbara Pasini[1] and Anna Sapino[1,2*]

Abstract

Background: The MCF7 (ER+/HER2-), T47D (ER+/HER2-), BT474 (ER+/HER2+) and SKBR3 (ER-/HER2+) breast cancer cell lines are widely used in breast cancer research as paradigms of the luminal and HER2 phenotypes. Although they have been subjected to cytogenetic analysis, their chromosomal abnormalities have not been carefully characterized, and their differential cytogenetic profiles have not yet been established. In addition, techniques such as comparative genomic hybridization (CGH), microarray-based CGH and multiplex ligation-dependent probe amplification (MLPA) have described specific regions of gains, losses and amplifications of these cell lines; however, these techniques cannot detect balanced chromosomal rearrangements (e.g., translocations or inversions) or low frequency mosaicism.

Results: A range of 19 to 26 metaphases of the MCF7, T47D, BT474 and SKBR3 cell lines was studied using conventional (G-banding) and molecular cytogenetic techniques (multi-color fluorescence *in situ* hybridization, M-FISH). We detected previously unreported chromosomal changes and determined the content and frequency of chromosomal markers. MCF7 and T47D (ER+/HER2-) cells showed a less complex chromosomal make up, with more numerical than structural alterations, compared to BT474 and SKBR3 (HER2+) cells, which harbored the highest frequency of numerical and structural aberrations. Karyotype heterogeneity and clonality were determined by comparing all metaphases within and between the four cell lines by hierarchical clustering. The latter analysis identified five main clusters. One of these clusters was characterized by numerical chromosomal abnormalities common to all cell lines, and the other four clusters encompassed cell-specific chromosomal abnormalities. T47D and BT474 cells shared the most chromosomal abnormalities, some of which were shared with SKBR3 cells. MCF7 cells showed a chromosomal pattern that was markedly different from those of the other cell lines.

Conclusions: Our study provides a comprehensive and specific characterization of complex chromosomal aberrations of MCF7, T47D, BT474 and SKBR3 cell lines.
The chromosomal pattern of ER+/HER2- cells is less complex than that of ER+/HER2+ and ER-/HER2+ cells. These chromosomal abnormalities could influence the biologic and pharmacologic response of cells. Finally, although gene expression profiling and aCGH studies have classified these four cell lines as luminal, our results suggest that they are heterogeneous at the cytogenetic level.

Keywords: Cytogenetic, Chromosomal abnormalities, Breast cancer cell lines, Hierarchical cluster

* Correspondence: anna.sapino@unito.it
[1]Department of Medical Sciences, University of Turin, Via Santena 7, 10126 Turin, Italy
[2]Department of Laboratory Medicine, Azienda Ospedaliera Città della Salute e della Scienza di Torino, Turin, Italy
Full list of author information is available at the end of the article

Background

The MCF7, T47D, BT474 and SKBR3 breast cancer cell lines are commonly used in experimental studies of cellular function, and much of the current knowledge of molecular alterations in breast cancer has been obtained from these cell lines [1-4].

Whole-genome studies using microarray expression analyses have identified distinct subtypes of breast carcinomas (the luminal, HER2+, and basal-like subtypes) based on the expression of approximately 500 genes (the so-called "intrinsic gene list") [5-7]. These molecular subtypes have been approximated using immunohistochemical markers. In this way, estrogen (ER) and progesterone receptor (PR)+/HER2- tumors are classified as belonging to the luminal A molecular subtype, ER+/PR+/HER2+ tumors to the luminal B subtype, ER-/PR-/HER2+ tumors to the HER2 subtype, and triple negative (ER-/PR-/HER2-) tumors to the basal-like carcinomas [8].

As determined by immunohistochemistry, the receptor profile classifies MCF7 and T47D cells (ER+/PR+/HER2-) as belonging to the luminal A subtype, BT474 cells (ER+/PR+/HER2+) as luminal B and SKBR3 cells (ER-/HER2+) as HER2 [9,10]. However, the RNA transcriptional profile determined by whole genome oligonucleotide microarrays [1,4,11] characterized all four-cell lines as luminal because of the expression of both ERα-regulated genes (e.g., MYB, RET, EGR3, and TFF1) [1] and genes associated with luminal epithelial differentiation (e.g., GATA3 and FOXA1).

Different works have assayed the DNA genetic profile of these cell lines using comparative genomic hybridization (CGH) and multiplex ligation-dependent probe amplification (MLPA) to describe many different copy number alterations [11-13]. With these techniques, however, balanced chromosome rearrangements (e.g., translocations or inversions) and low frequency mosaicism (< 30% abnormal cells) are not detectable. These chromosomal alterations may be assessed on metaphases using G-banding karyotype and multicolor fluorescence *in situ* hybridization (M-FISH) [2,12-16]. However, because both procedures are time consuming, they have been applied to only a small number of metaphases [2,12-17]. Thus, to our knowledge, a search for clonal chromosomal aberrations within each cell line [2,12-16] and a comprehensive comparison of the MCF7, T47D, BT474 and SKBR3 cell lines from a cytogenetic perspective have not yet been performed.

In the present study, we evaluated structural and numerical alterations on a large number of metaphases of MCF7, T47D, BT474 and SKBR3 breast cancer cell lines using a combination of G-banding and M-FISH. This allowed us to analyze cell clonality within each cell line and to thoroughly compare the cytogenetic of the cell lines by clustering analysis.

Results

Between 19 and 26 metaphases with good chromosome dispersion and morphology were analyzed for each cell line to define the structural and numerical alterations, and 100 metaphases/cell line were analyzed to determine the level of ploidy. The rate and type of chromosomal abnormalities for each cell line are shown in Figure 1.

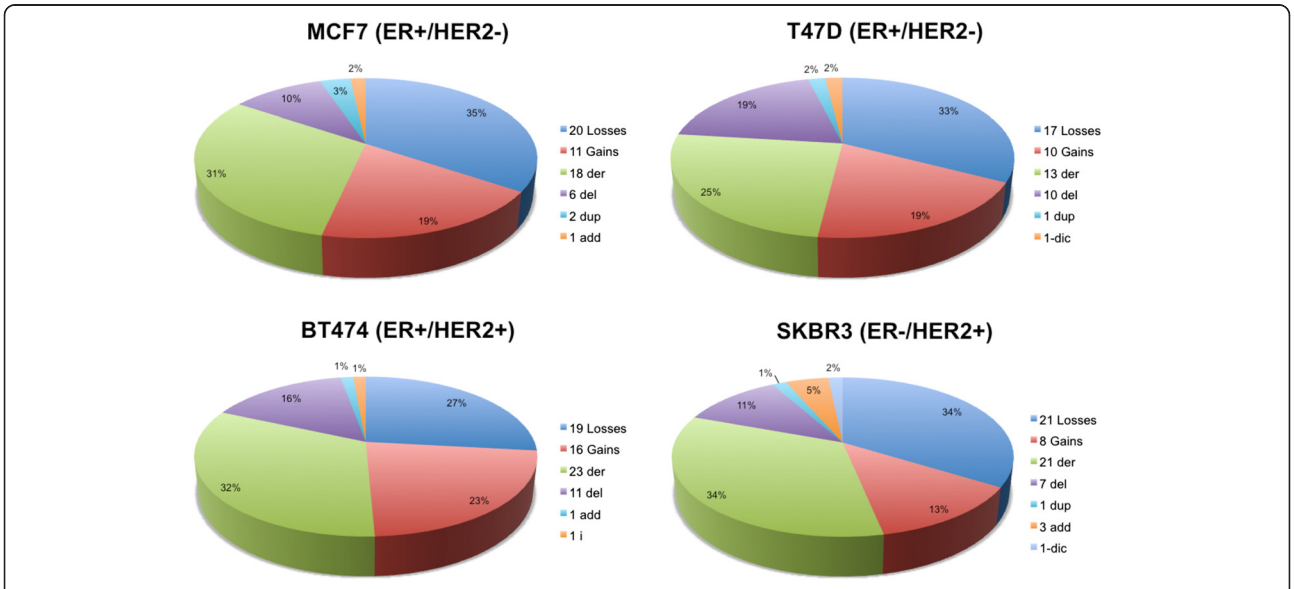

Figure 1 Distribution of numerical and structural aberrations across the four breast cancer cell lines. der = derivative chromosome; del = deletion; dup = duplication; add = additional material of unknown origin; dic = dicentric chromosome.

Cytogenetic profile and cluster analysis of MCF7 cells

The cytogenetic analysis performed on 26 metaphases of MCF7 cells demonstrated a modal number hypertriploid to hypotetraploid (4n+/−) (76 to 88 chromosomes). Each chromosome harbored either a numerical or structural aberration, which accounted for 58 different rearrangements (31 numerical and 27 structural). Polyploidy was observed in 2% of the cells. Numerical alterations were present in all chromosomes; losses were more frequent than gains (Figure 1). Chromosomes 18 and 20 were nullisomic in 11.5% and 30.7% of the cells, respectively. Structural aberrations (translocations, duplications and deletions) were found in all chromosomes except 4, 5, 13, 14 and 18.

A cluster analysis indicated that the types of chromosomal alterations were similar in the 26 metaphases (horizontal dendrogram, Figure 2). Clustering by the frequency of the chromosomal aberration within a cell line produced 4 clusters (vertical dendrogram, Figure 2). The first cluster (red bar) represented chromosomal alterations that were frequently present; chromosome 7 was the most affected by structural abnormalities. The second cluster (blue bar) represented alterations that were present in all metaphases, including chromosome losses and structural alterations of chromosomes 8 and 17. In particular, the loss of chromosomes 11, 18, 19 and 20 and the gain of chromosomes 7 and 17 were observed in all metaphases.der(6)t(6;17;16)(q25;q21;?), der(8)t

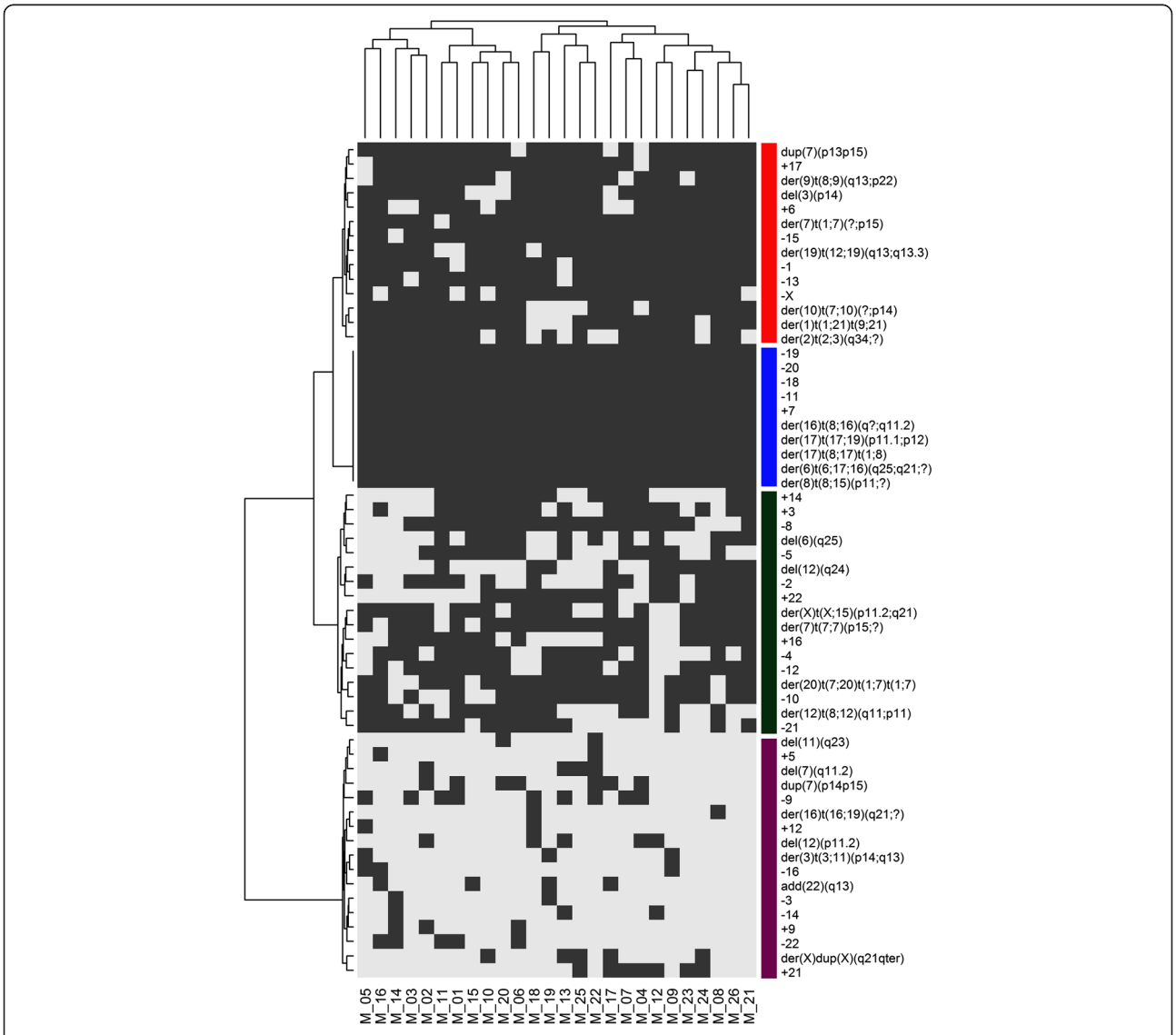

Figure 2 Hierarchical cluster analysis of the presence or absence of chromosomal aberrations observed in 26 MCF7 metaphases. Each column refers to a metaphase (M) and each row to a chromosomal abnormality. Grey indicates the presence of each abnormality, and white indicates their absence. The cluster number is indicated by vertical color bars. Cluster 1: red bar, cluster 2: blue bar, cluster 3: green bar and cluster 4: purple bar.

Table 1 G-Banding and M-FISH karyotypes of all breast cancer cell lines studied

Cell line	Karyotype
MCF7	76 ~ 88 < 4n>,-X[11],-Xx2[8],-Xx3[4],der(X)t(X;15)(p11.2;q21)[16],
	der(X)t(X;15)(p11.2;q21)x2[3],der(X)dup(X)(q21qter)[5],-1[22]-1x2[2], der(1)t(1;21)t(9;21)[22],-2[13], -2x2[2],der(2)t(2;3)(q34;?)[19],-3[2],
	+3[17],del(3)(p14)[22],der(3)t(3;11)(p14;q13)[3],-4[12],-4x2[4],
	+5[2],-5[13],+6[9],+6x2[8],+6x3[4],add(6)(q27)[2],del(6)(q25)[4],
	del(6)(q25)x2[8], der(6)t(6;17;16)(q25;q21;?)[26],
	+7[26],der(7)t(1;7)(?;p15)[23],der(7)t(1;7)(?;p15)x2[2], del(7)(q11.2)[4],dup(7)(p13p15)[7],dup(7)(p13p15)x2[5], dup(7)(p13p15)x3[11],dup(7)(p14p15)[5],dup(7)(p14p15)x2[2],der(7)t(7;7)(p15;?)[19], der(7)t(7;7)(p15;?)[2],-8[8], -8x2[12],der(8)t(8;15)(p11;?)[26],+9[3]
	−9[7],-9x2[2],der(9)t(8;9)(q13;p22)[22],-10[6],-10x2[10],-10x3[3],
	der(10)t(7;10)(?;p14)[9],der(10)t(7;10)(?;p14)x2[12],-11[14],
	−11x2[12],del(11)(q23)[2],-12[15],-12x2[4],+12[2],
	del(12)(p11.2)(5),del(12)(q24)[11],der(12)t(8,12)(q11;p11)[15],
	−13[12],-13x2[10],-13x3[2],-14[3],+14[14],-15[12],-15x2[10],
	−15x3[3],-16[3],+16[16],der(16)t(8;16)(q?;q11.2)[8],der(16)t(8;16)(q?;q11.2) x2[17]der(16)t(16;19)(q21;?)[2], +17[11],+17x2[10],+17x3[5],der(17)t(8;17)t(1;8)[21],der(17)t(8;17)t(1;8)x2[5],der(17)t(17;19)(p11.1;p12)x2[17],-18[4],
	−18x2[14],-18x3[5],-18x4[3],-19[7],-19x2[15],-19x3[4],
	der(19)t(12;19)(q13;p13.3)[21],der(19)t(12;19)(q13;p13.3)x2[2],-20[2],
	−20x2[5],-20x3[11],-20x4[8],der(20)t(7;20)t(1;7)t(1;7)[21],+21[5],+21x2[2],-21[14],-21x2[2],+22[12],+22x2[3],-22[3], -22x2[2],add(22)(q13)[4][cp26]
T47D	57 ~ 66 < 3n>,X,-X[24],der(X)t(X;6)(q12;p11)[24],-1[19],-2[22],
	−3[5],del(3)(p11)[2],del(3)(p14)[2],del(3)(p21)[2],del(3)(q13)[6],del(3)(q22)[3],
	der(3)ins(3;5)(p14;q13q31)[2],der(3)del(3)(p13)del(3)(q13q25)ins(3;5)(q13;q13q31)[2],
	−4[19],-5[2],+5[3],-6[17],+7[3],del(7)(p21)[3],del(7)(p13p14)[5], del(7)(p13p14)x2[10],del(7)(p13p15)[8], der(7)t(7;15)(q21;q13)[3],dup(7)(p13p14)[2],+8[12],der(8;14)(q10;q10)x2[24],-9[11],-9x2[9],-10[11],-10x2[10], del(10)(p10)[3], der(10)t(3;10)(q?;q24)del(10)(p11.2)[14],der(10)t(3;10)(q?;q24)del(10)(p11.2)x2[10],+11[9], +11x2[7],+11x3[2],der(11)t(11;17)(q23;q?)t(9;17)(q?12;?)[2],-12[2],+12[6],+12x2[4],
	del(12)(p12)[6],del(12)(q24.1)[5],del(12)(q24.1)x2[3],der(12)del(12)(p12)del(12)(q24)[4],
	der(12)t(12;13)(p12;q22)[10],der(12)t(12;16)(p11.2;?)[11],-13[16],-13x2[4],+14[3],+14x2[13],
	+14x3[3],-15[6],-15x2[18],-16[2],der(16)t(1;16)(q12;q12)dup(1)(q21q43)[24],
	dic(9;17)t(9;17)(p12;p13)[13],dic(9;17)t(9;17)(p12;p13)x2[11],-18[17],-18x2[4],-19[18],
	+20[9],+20x2[3],der(20)t(10;20)(q21;q13.3)[15],der(20)t(10;20)(q21;q13.3)x2[9],der(20)del(20)(p11)t(10;20) (q21;q13.3)[10],+21[10],+21x2[6],-21[2], -22[14][cp24]
BT474	65 ~ 106 < 4n>,X,-X[9],-Xx2[5],-Xx3[4],der(X)t(X;17)(q13;q11q12)del(X)(p21)
	[9],der(X)t(X;18;X;12)[2],del(X)(q22)[14],-1[6],-1x2[2],+1[3],del(1)(p36.1)[6], -2[7],+2[7],der(2)t(1;2;7;20)(?;q31;?;?) [18],+3[12],-3[3],del(3)(p11.2)[7],
	del(3)(p14)[2],del(3)(q11.2)[6],del(3)(q11.2)x2[8],del(3)(q21)[4],del(3)(q13)[2],
	−4[8],-4x2[9],+4[2],-5[9],-5x2[9],+6[11],+6x3[3],-6[3],
	del(6)(q13)[3],del(6)(q21)[3],der(6)t(6;7)(q25;q31)[7],der(6)t(6;7)(q25;q31)x2[16],+7[4],+7x2[6],+7x3[9],+7x4[3], der(7)t(7;20)(p13;?)[5], der(7)t(1;7)(?;q11.2)[9],
	del(7)(q11.2)[7],del(7)(q11.2)x2[3],del(7)(q11.2)x3[3],der(7)t(7;14)(p13;p11.2)[4],-8[10], -9[7],-9x2[4],-9x3[2], der(9)t(3;9)(q33;?)[3],+10[6],-10[5],
	der(10)t(10;16;19)(q25;?;?)[11],i(10)(q10)[4],+11[9],+11x2[2],-11[3],
	der(11)t(8;11)(q21.1;p15)[2],der(11)t(8;17)(q21.1;q11q12)t(11;17)(p15;q11q12)[8],der(11)t(8;17)(q21.1; q11q12)t(11;17)(p15;q11q12)x2[12],der(11)t(8;17)(q21.1;q11q12)t(11;17)(p15;q11q12)x3[3],der(11)t(11;17) (q?14;?)t(8;17)(?;q?11.2)[13], der(11)t(11;17)(q?14;q?11.2)[9],+12[8],
	+12x2[5],del(12)(p11.1)[2],der(12)t(5;12)(q23;q23)[17],der(12)t(5;12)(q23;q23)x2[2],der(12)del(12)(p12)del (12)(q24)[3],-13[7],+13[6],+13x2[3],+13x4[2],
	der(13)t(13;17)(q10;q11q12)t(13;17)(q10;q11q12)

Table 1 G-Banding and M-FISH karyotypes of all breast cancer cell lines studied *(Continued)*

	[8],der(13)t(13;17)(q10;q11q12)t(13;17)(q10;q11q12)x2[12],+14[11], +14x2[3],+14x3[2],der(14)t(14;1;14)(q31;?;?)[6],der(14)t(14;1;14)(q31;?;?)x2[5],
	der(14)t(14;1;14)(q31;?;?)x3[9],der(14)t(14;1;14)(q31;?;?)x4[3],
	add(14)(p11.2)[2],der(14;14)(q10;q10)[3],der(14;14)(q10;q10)x2[16],-15[6],-15x2[9], -15x3[6],+16[7],+16x2[6], +16x3[3],-16[2],der(16)t(X;16)(q22;q24)[10],
	+17[16], der(17)t(6;17)(?;p13)t(15;17)(q11.2;q25)[22],-18[10],-18x2[4],-18x3[2],-19[6],
	−19x2[5],+19[5],-20[6],-20x2[6],+20[3],+20x3[2],der(20)t(19;20)(?;q10)[4],
	der(20)t(19;20)(?;q10)x2[5],+21[2],-21x2[11],-21x3[3],-22[2],-22x2[5],-22x3[2],-22x4[12],
	der(22)t(16;22)(q12;p11.2)[5][cp23]
SKBR3	76 ~ 83 < 4n>,XXX,-X[19],der(X)t(X;17)(q21;q?21)[15], der(X)t(X;8;17)(q13;q?21;?)[6],+1[8],+1x3[5],add(1)(p36.3)[4],
	del(1)(p13)[11],del(1)(p13)x2[6],del(1)(p34)[4],del(1)(p22)[9],del(1)(p36.1)[2], der(1)t(1;4)(q12;q12)[6],-2[6],-2x2[8], -2x3[3],der(2)t(2;6)(p13;?)[5],-3[10],-3x2[6],-4[8],
	−4x2[8],-4x3[3],der(4;14)t(4;14)(p11;p11.1)[3],-5[8],
	−5x2[8],-5x3[2],der(5)ins(5;15)(p13;q12q22)[6],-6[4],-6x2[12],
	−6x3[2],der(6)t(6;14;17)(q21;?;q11q12)del(6)(p23)[8],+7x2[8],+7x3[10],
	del(7)(q22)[12],del(7)(q32)[3],dup(7)(p14p15)[2],-8[6],+8[8],
	der(8)t(8;21)(?;?)t(8;21)(p23;?)t(8;21)(q24;?)[11],der(8)t(8;21)(?;?)t(8;21)(p23;?)t(8;21)
	(q24;?)x2[8],der(8)dup(8)(?)t(8;8)(?;p23)t(8;17)(q24;?)t(11;17)(?;?)[4],
	der(8;14)t(8;14)(p11.1;p11.1)[15],-9[9],-9x2[7],-10[4],-10x2[13],-10x3[2],+11[2],-11[7],
	add(11)(p15)[4],add(11)(q25)[2],-12[6],-12x2[5],+12[3],der(12)t(11;12)(p?;p12)[4],
	der(12)t(5;12)(q23;q23)[10],der(12)t(5;12)(q23;q23)x2[4],-13[6],-13x2[8],
	−13x3[3],der(13;13)(q11.2;q11.2)[16],-14[6],-14x2[4],
	der(14;14)(q11.2;q11.2)[18],-15[10],-15x2[7], dic(15;21)(p11.1;p11.1)[3],
	+16[4],-16[7],-17[3],+17[9],der(17;17)t(17;17)(q25;?)dup(17)(q22q25)t(17;20)(?;?)[5],
	der(17;17)t(17;17)(q25;?)dup(17)(q22q25)t(17;20)(?;?)x2[7], der(17;17)t(17;17)(q25;?)dup(17)(q22q25)t(17;20)(?;?)x3[7],del(17)(p11.2)[7],
	der(17)t(8;17)(q12;?)dup(17)(?)[19],der(17)t(8;17)(?;q25)dup(17)
	(q22q25)[5],der(17)t(8;17)(?;q25)dup(17)(q22q25)x2[2],der(17)t(8;13;14;17;21)(?;q?;q?;q11q12;?)[8], der(17)t(3;8;13;17;20)(?;?;q12;?p;?)[12],der(17)t(3;8;13;17;20)(?;?;q12;?p;?)x2[2],-18[3],-18x2[11],-18x3[5], der(18)t(18;22)(p11.2;?)[12],-19[4],-19x2[7],-20[8],-20x2[4],
	−20x3[7],-21[6],-21x2[3],-22[9],-22x2[4],+22[2],der(22)t(19,22)(q?;q13)[5][cp19]

The number of metaphases analyzed is reported in brackets at the end of each karyotype. Additionally, the frequency of each rearrangement identified is described in brackets.

(8;15)(p11;?), der(16)t(8;16)(q?;q11.2), der(17)t(8;17)t(1;8) and der(17)t(17;19)(p11.1;p12) were present in all cells as a consequence of structural aberrations (Table 1 and Figure 3A and 3B).

Less frequent alterations (mainly numerical) constituted cluster 3 (green bar), and very rare alterations (ranging from 0 in metaphases M_21 and M_26 to 5 in metaphases M_13 and M_22) constituted cluster 4 (purple bar).

Cytogenetic profile and cluster analysis of T47D cells

In the T47D cells, 24 metaphases were examined. The modal number was near triploidy (3n+/−) (57 and 66 chromosomes). T47D cells had 52 different chromosomal alterations (27 numerical and 25 structural) (Figure 1). Polyploidy was observed in 4% of the analyzed cells, and numerical chromosomal alterations were present in all chromosomes. Structural aberrations (deletions, translocations, and duplications) were found in all chromosomes except 2, 4, 18, 19, 21 and 22.

As in the MCF7 cells, the types of chromosomal alterations were almost homogeneously distributed among the 24 metaphases of T47D cells, as demonstrated by hierarchical clustering (horizontal dendrogram, Figure 4). When the frequency of chromosomal alterations was analyzed, 3 clusters were identified (vertical dendrogram): the first and largest cluster (red bar) was formed by common numerical alterations with a prevalence of losses. The rare structural aberrations present in this cluster primarily involved chromosome 12. In the second cluster (the smallest, blue bar), der(X)t(X;6)(q12;p11), der(8;14)(q10;q10), der(10)t(3;10)(q?;q24)del(10)(p11.2), der(16)t

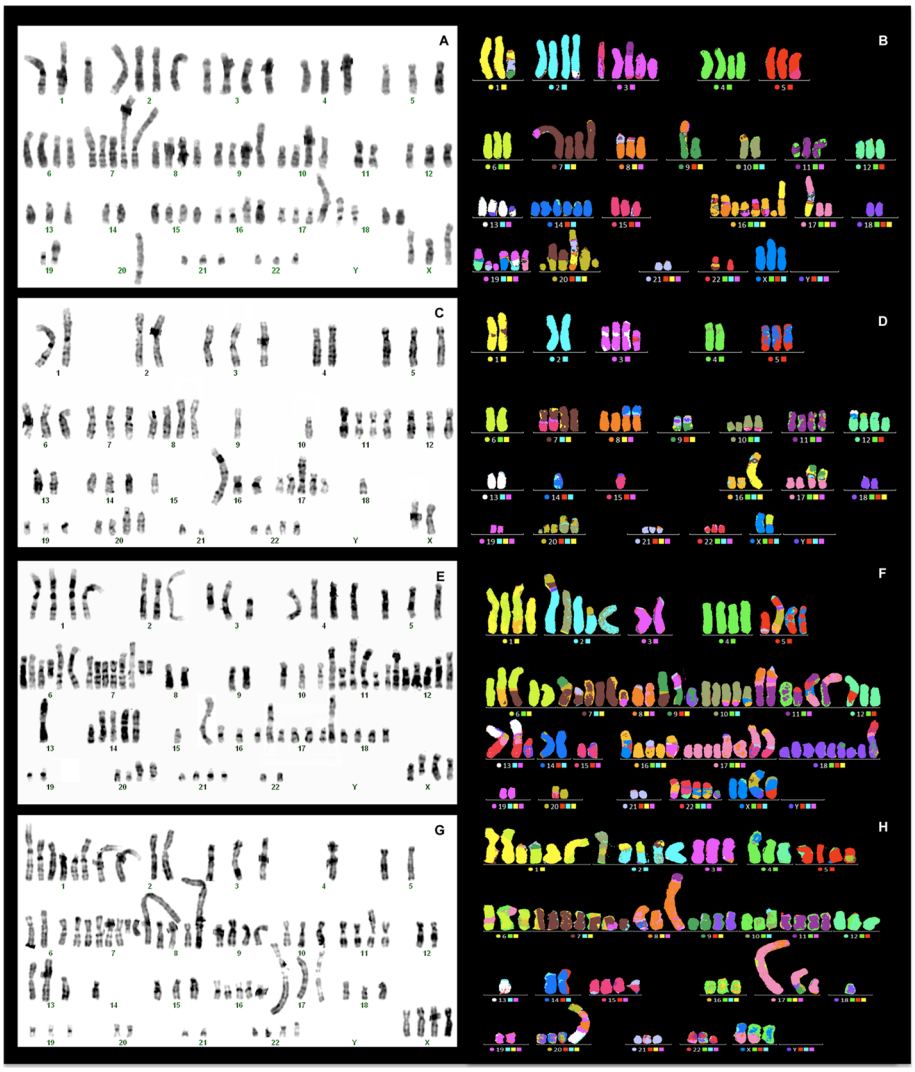

Figure 3 G-Banding and molecular cytogenetic results of four breast cancer cell lines. A-B) G-banded and M-FISH karyotype of a representative metaphase of MCF7 cells. **C-D)** G-banded and M-FISH karyotype of a representative metaphase of T47D cells. **E-F)** G-banded and M-FISH karyotype of a representative metaphase of BT474 cells. **G-H)** G-banded and M-FISH karyotype of a representative metaphase of SKBR3 cells.

(1;16)(q12;q12)dup(1)(q21q43), dic(9;17)t(9;17)(p12;p13) and der(20)t(10;20)(q21;q13.3) were present in all metaphases as the result of translocations, together with the loss of chromosomes 15 and X (Table 1 and Figure 3C and 3D). Cluster 3 (green bar) grouped rare abnormalities (ranging from zero in metaphases M_17 and M_21 to 4 in metaphases M_11 and M_10), most of which were structural (Figure 4).

Cytogenetic profile and cluster analysis of BT474 cells

For BT474 cells, 23 metaphases were examined. These cells showed the highest frequency of numerical and complex structural aberrations of all cell lines analyzed. BT474 cells had a modal number near tetraploidy (4n+/−) (from 65 to 106 chromosomes) and showed 35 numerical and 36 structural aberrations (Figure 1). Polyploidy was not present.

As in the other cell lines, cluster analysis demonstrated nearly homogeneous chromosome alterations in all metaphases (horizontal dendrogram, Figure 5). Isochromosomes, deletions and derivatives were frequent (Table 1 and Figure 3E and 3F). Numerical alterations were also observed in all chromosomes, with losses being more frequent than gains. Losses of chromosomes X, 15 and 22 were observed in 78%, 91% and 91% of metaphases, respectively, while gain of chromosome 7 was identified in 96% of cells.

The frequency of alterations within the cell line produced 2 clusters (vertical dendrogram): in cluster 1 (red bar), both numerical and structural alterations

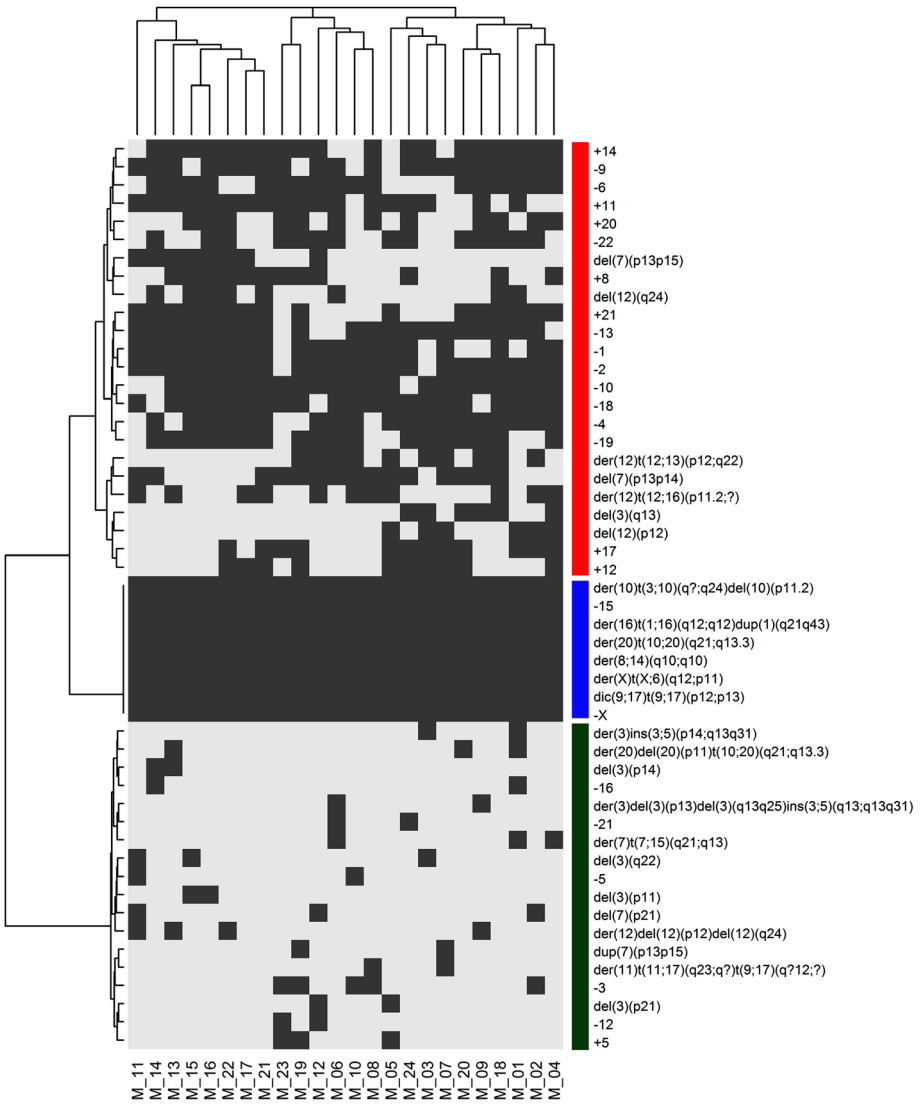

Figure 4 Hierarchical cluster analysis of the presence or absence of chromosomal aberrations observed in 24 T47D metaphases. Each column refers to a metaphase (M) and each row to a chromosomal abnormality. Grey indicates the presence of each abnormality, and white indicates their absence. The cluster number is indicated by vertical color bars. Cluster 1: red bar, cluster 2: blue bar and cluster 3: green bar.

were present in almost all cells. Only three structural alterations were reproduced in all metaphases, namely der(6)t(6;7)(q25;q31), der(11)t(8;17;11)(q21.1;?;p15) and der(14;1;14)(q31;?;?) (Table 1 and Figure 3E and 3F). Cluster 2 (blue bar) included sporadic aberrations with a minimum of 3 such alterations observed in metaphase M_22 (Figure 5).

Cytogenetic profile and cluster analysis of SKBR3 cells

In this cell line, 19 metaphases were examined. SKBR3 cells showed a hypertriploid to hypotetraploid (4n+/−) (76 to 83 chromosomes) karyotype. Polyploidy was observed in 19% of all cells. SKBR3 cells had 29 numerical and 33 structural aberrations (Figure 1). Numerical chromosomal alterations were observed in all chromosomes. Structural aberrations (translocations, deletions, and duplications) were found in all chromosomes except 3, 9, 10 and 16 (Table 1 and Figure 3G and 3H).

In comparison to other cell lines, hierarchical clustering showed similarities of chromosomal alterations among the 19 metaphases (horizontal dendrogram, Figure 6). Clustering by the frequency of chromosomal alterations defined 3 clusters (Figure 6). The largest cluster (cluster 1, red bar) was formed by sporadic aberrations, with structural aberrations being prevalent. Cluster 2 (blue bar) included frequent rearrangements, with more numerical than structural aberrations. The smallest group (cluster 3, green bar) contained chromosomal abnormalities that were present

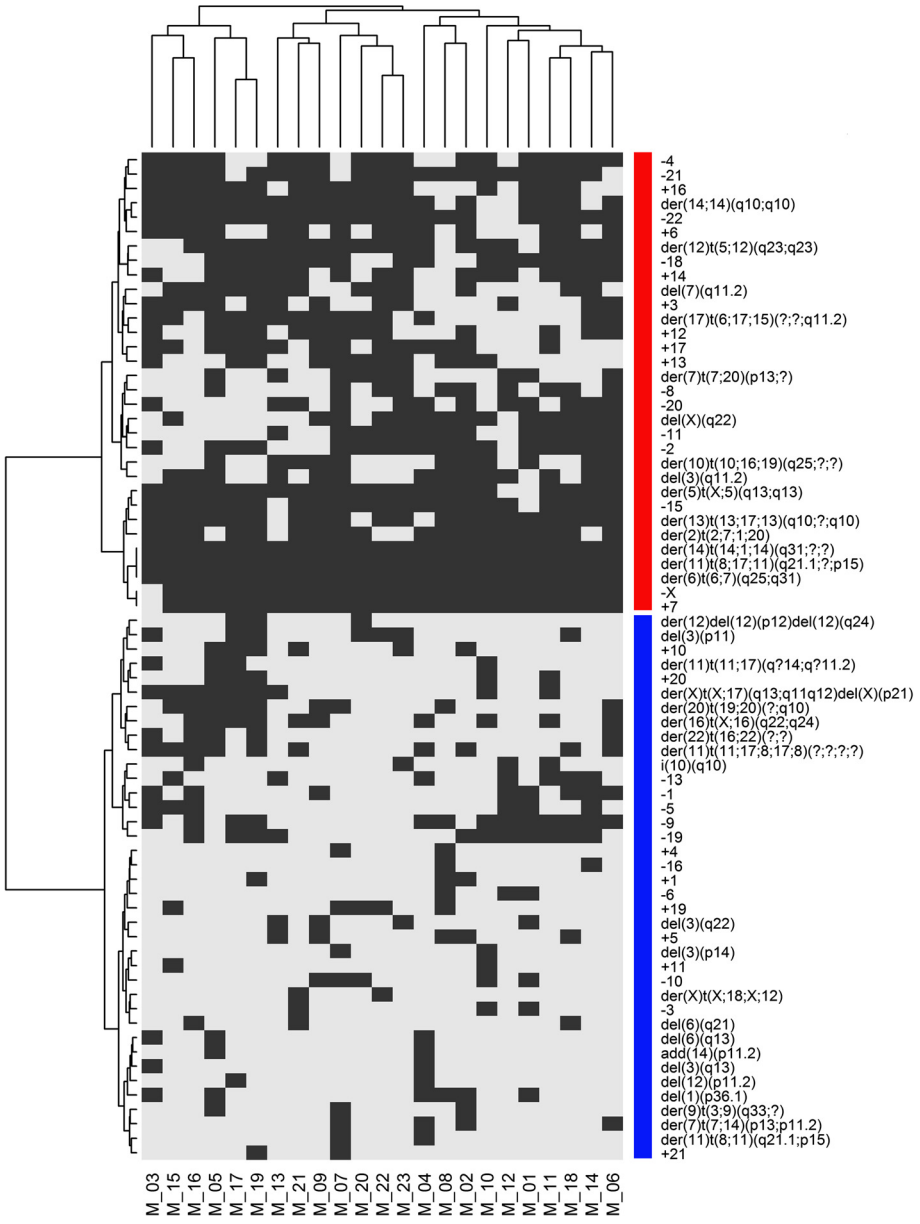

Figure 5 Hierarchical cluster analysis of the presence or absence of chromosomal aberrations observed in 23 BT474 metaphases. Each column refers to a metaphase (M) and each row to a chromosomal abnormality. Grey indicates the presence of each abnormality, and white indicates their absence. The cluster number is indicated by vertical color bars. Cluster 1: red bar and cluster 2: blue bar.

in all cells, both numerical, such as monosomies of chromosomes X, 4, 10, 18 and 20, and structural, such as those on chromosomes 8, 17 and 1.

Comparison of the four cell lines

Using hierarchical clustering, we identified five major clusters (Figure 7). One cluster was characterized mainly by numerical chromosome abnormalities (18 losses and 7 gains) that were common to the four cell lines. Only two structural alterations, namely der(14;14)(q10;q10) and der(12)t(5;12)(q23;q23), were common to HER2+ cells. The other clusters, however, encompassed cell type-specific abnormalities that were primarily structural (Figure 7). This analysis revealed greater similarity between T47D and BT474 cells and some similarity between these two cell lines and the SKBR3 cell line. MCF7 cells demonstrated a chromosome pattern that was markedly different from those of the other lines (Figure 8).

Discussion

The MCF7 (ER+/HER2-), T47D (ER+/HER2-), BT474 (ER+/HER2+) and SKBR3 (ER-/HER2+) cell lines are

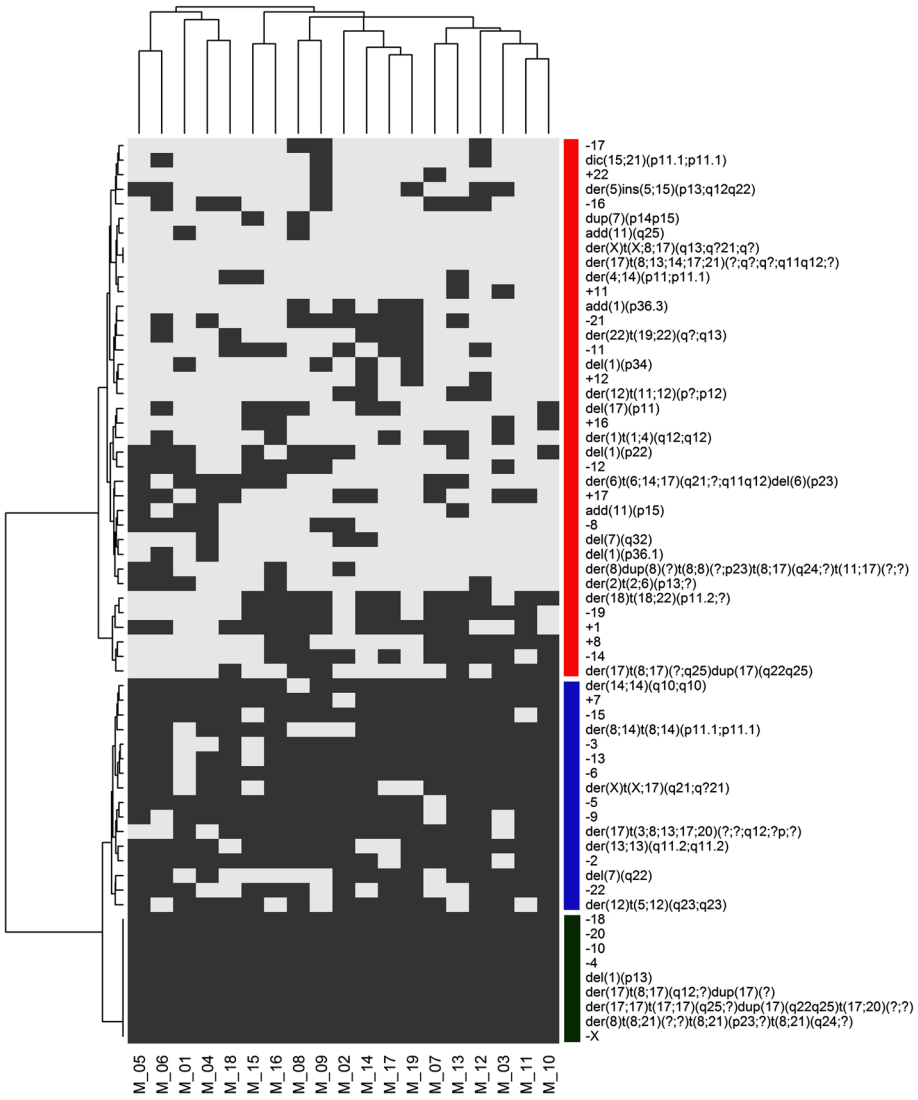

Figure 6 Hierarchical cluster analysis of the presence or absence of chromosomal aberrations observed in 19 SKBR3 metaphases. Each column refers to a metaphase (M) and each row to a chromosomal abnormality. Grey indicates the presence of each abnormality, and white indicates their absence. The cluster number is indicated by vertical color bars. Cluster 1: red bar, cluster 2: blue bar and cluster 3: green bar.

widely used in breast cancer research as paradigms of the luminal and HER2 immunophenotypes [9,10]. Although classical cytogenetic analysis is time consuming and lacks the resolution of molecular techniques, it is the best tool for obtaining an overall picture of the types and frequency of chromosome changes. The results obtained using G-Banding and M-FISH analyses of a large number of metaphases allowed us to acquire a thorough insight of the type and frequency of chromosome alterations in the MCF7, T47D, BT474 and SKBR3 cell lines and to detect previously unreported chromosome alterations (Table 2).

Cluster analysis excluded the presence of cell clones within each cell line because the same abnormalities were homogenously observed in all metaphases. Conversely, within the same cell line, the frequency of each chromosome alteration was variable and defined different clusters. Finally, a comparison of these four cell lines using cluster analysis showed that they shared up to 5 numerical aberrations in more than 50% of the metaphases (−2, -4, -15, -18, -X) and that the chromosomal structural alterations were cell-type specific, with the exception of two derivative chromosomes that were shared by the BT474 and SKBR3 HER2+ cell lines.

The HER2+ cell lines BT474 and SKBR3 showed the highest frequency of numerical and structural aberrations in comparison with the HER2- cell lines MCF7 and T47D. Polyploidy, which was more frequent in HER2+ than in HER2- cells, has been correlated with short survival, drug resistance and metastasis [19]. In addition, complex

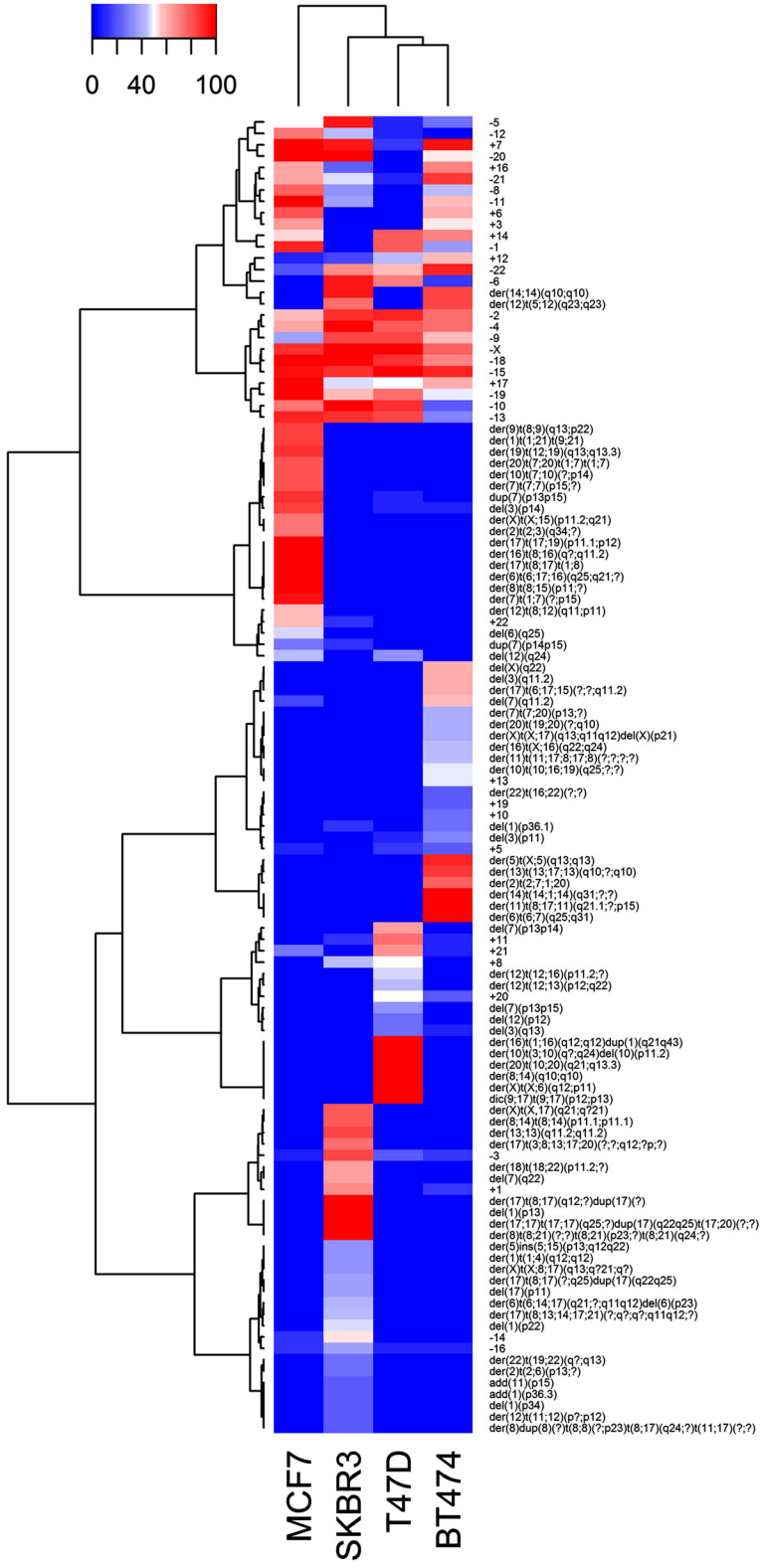

Figure 7 Hierarchical cluster analysis of the percentage of chromosomal aberrations observed in four breast cancer cell lines. Clustering stratifies cell lines into five groups. The first cluster was characterized by the presence of numerical chromosomal abnormalities (aneuploidies) that were common to the four cell lines (ER+, ER-, HER2+, HER2-). The other clusters comprised cell type-specific chromosomal abnormalities. The gradient color indicates percentage of chromosomal abnormalities present in each cell line.

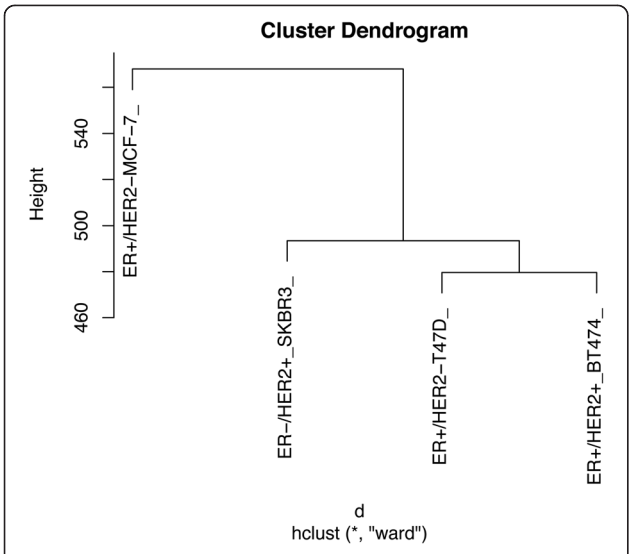

Figure 8 Cluster dendrogram derived from cytogenetic analysis of the four breast cancer cell lines. These analyses confirmed the greater similarities between T47D and BT474 cell lines and between these two cell lines and the SKBR3. MCF7 cells demonstrate a chromosomal pattern that was markedly different from those of previous cells.

chromosome alterations affecting chromosomes 8, 11, and 17 were frequently observed in HER2+ cells. These chromosomes contain genes that are commonly involved in the invasion, metastasis and pathogenesis of breast cancer, including *c-MYC* on 8q24; *HRAS, CD151, CTSD* on 11p15; *CCND1* on 11q13 [20-24]; and *TOP2A* on 17q21. Moreover, in HER2+ cells and carcinomas, rearrangements of chromosome 17 are more frequent than is polysomy. Pathologists must consider this observation for when diagnosing the HER2 amplification in interphase nuclei of breast carcinomas, which uses a ratio between HER2 copies and chromosome 17 centromere signals [25,26].

Among ER + cells, MCF7 cells are cytogenetically different than both T47D (ER+/HER2-) and BT474 (ER+/HER2+) cells and are characterized by a specific subset of complex structural alterations, which are listed in the cluster analysis comparison of the four cell lines (Figure 7). In particular, chromosome 7 was frequently structurally and numerically affected, and polysomy of chromosome 7 was observed in all metaphases. This finding has been closely associated with lymph node metastasis and prognosis in breast cancer patients [27]. One may speculate that the differences observed in the pattern of chromosomal aberrations between the MCF7 and T47D cell lines could partly explain the differences in the profile of protein expression that was recently identified in these cells [28]. Proteomic studies have revealed that a high number (at least 164) of proteins (including proteins involved in the regulation of breast cancer cell growth) are differentially expressed by T47D and MCF7 cells [28]. For example, of the proteins that are principally involved in cell proliferation and apoptosis and are upregulated in MCF7 cells, the Chromobox protein homolog 3 and the Cytochrome c-releasing factor 21 are encoded by genes mapping to chromosome 7, which is typically polysomic in MCF7 cells, as reported above. The differences in the karyotype should be considered when designing related experimental studies, such as those that analyze the effect of gene transfection. It is possible that complex chromosome alterations may alter the results. MCF7 cells, which differ greatly from the BT474 and SKBR3 (HER2+) cells, are frequently used to study the effect of HER2 transfection [29-31]; however, they may not represent the best substrate. Conversely, T47D cells (ER+/HER2-) and BT474 cells share similarities in the chromosome profile, and both have some chromosomal similarities with SKBR3 cells. For example, T47D and BT474 cells share numerical alterations, such as losses of chromosome 6 and gains of chromosomes 11 and 20, but they have no structural abnormalities in common.

One may hypothesize that the earliest genetic event may be aneuploidy, followed by structural alterations [32,33]. Aneuploidy is one of the most common properties of cancer [34]. In addition, numerical abnormalities have been observed more frequently in primary cancers, while structural alterations and amplifications were more commonly observed in metastatic breast cancer [33]. These structural alterations may lead to the deregulated expression of genes, such as a loss of tumor suppressor genes, the activation of oncogenes and the formation of fusion proteins with enhanced or aberrant transcriptional activity. For instance, some of the genes upregulated in HER2+ cell lines [35] reside on chromosomes 5, 6, 10, 19, and 20, which were reported to be polysomic in BT474 cells in the present study (Additional file 1: Table S1).

Conclusions

In conclusion, by using both conventional and molecular karyotyping, our work provides a comprehensive and specific characterization of complex chromosomal aberrations for MCF7, T47D, BT474 and SKBR3 cell lines, thus providing important information for experimental studies. These cell lines serve as models for investigating the molecular biology of breast cancer; therefore, it may be essential to consider the potential influence of these chromosomal alterations when interpreting biological data.

Methods

Cell lines

The human breast cancer cell lines MCF7 (ER+/HER2-), T47D (ER+/HER2-), BT474 (ER+/HER2+) and SKBR3 (ER-/HER2+) were obtained from the American Type Culture Collection (ATCC, Manassas, VA, USA) in

Table 2 Comparison of selected chromosomal aberrations detected in MCF7, T47D, BT474 and SKBR3 cell lines in previous studies and in our G-banding and M-FISH results

Cell line	ATCC	National Center for Biotechnology Formation NCBI [18]	Gasparini, et al. 2010 [15]	Davidson, et al. 2000 [14]	G-banding and M-FISH present study
MCF7	NR	NR	dup(X)(?;qter)	der(1)t(X;1)	der(X)dup(X)(q21qter)
	NR	NR	NR	NR	der(6)t(6;17;16)(q25;q21;?)
	NR	der(17)t(17;20)(q25;?)t(1;20)t(1;3or7)	NR	der(?)t(11;1;17;19;17)	der(17)t(17;19)(p11.1;p12)
	NR	NR	NR	der(?)t(17;1;19;17;20)	der(17)t(8;17)t(1;8)
T47D	der(8)t(8;14)	der(8)t(8;14)(p21;q21)	_	der(8)t(8;14)	der(8;14)(q10;q10)
	der(9)t(9;17)	der(9)t(9;17)(p12;q?11)	_	NR	dic(9;17)t(9;17)(p12;p13)
	der(10)t(10;20)	der(20)t(10;20)(q21;q13)	_	NR	der(20)t(10;20)(q21;q13.3)
BT474	der(6)t(6;7)(q21;q21)	_	der(6)t(6;7)(q25;?)	_	der(6)t(6;7)(q25;q31)
	NR	_	der(11)t(8;11;??)(?;p15;?)	_	der(11)t(8;17;11)(q21.1;?;p15)
	NR	_	NR	_	der(11)t(11;17)(q?14;q?11.2)
	i(13q)	_	der(13;13)(q10;q10)	_	der(13)t(13;17;13)(q10;?;q10)
	der(14)t(14;?)(q32,?)	_	der(14)t(1;14;X)(?;q31;?)	_	der(14)t(14;1;14)(q31;?;?)
SKBR3	NR	_	NR	der(8)t(8;21)	der(8)t(8;21)(?;?)t(8;21)(p23;?)t(8;21)(q24;?)
	NR	_	NR	NR	der(8)dup(8)(?)t(8;8)(?;p23)t(8;17)(q24;?)t(11;17)(?;?)
	NR	_	NR	der(?)t(8;14)	der(8;14)t(8;14)(p11.1;p11.1)
	NR	_	NR	NR	der(17)t(8;17)(q12;?)dup(17)(?)
	NR	_	NR	der(?)t(20;19;8;17)	der(17;17)t(17;17)(q25;?)dup(17)(q22q25)t(17;20)(?;?)
	NR	_	NR	der(8?)t(13;3;8;3;8;13)	der(17)t(8;13;14;17;21)(?;q?;q?;q11q12;?)
	NR	_	NR	der(?)t(20;3;8;17;19;8;3;13)	der(17)t(3;8;13;17;20)(?;?;q12;?p;?)
	NR	_	NR	NR	der(17)t(8;17)(?;q25)dup(17)(q22q25)
	NR	_	NR	der(?)t(19;22)	der(22)t(19,22)(q?;q13)

Abbreviations: NR, not reported. Dashes indicate that no information was available.

March 2010. Short tandem repeat (STR) analysis is routinely performed by ATCC during both accessioning and culture replenishment to avoid distributing misidentified cell lines to the scientific community. When received by our lab, these cell lines were expanded, and 3 vials were immediately frozen. Cells obtained from these stocks were used for the experiments. The cell lines were further authenticated based on the expression of epithelial markers (keratins 8 and 18) and the presence of specific receptors (ERα, PGR, HER2, AR and EGFR) using quantitative PCR (qPCR) and immunohistochemical analysis. The expression status of ERα and HER2 was further confirmed by western blot.

MCF7, T47D, and SKBR3 cells were cultured in RPMI 1640 medium (Sigma, St. Louis, MO, USA), while BT474 cells were cultured in DMEM medium (Sigma). Culture media were supplemented with 10% fetal bovine serum (FBS) (Sigma), antibiotic-antimycotic solution (1X) (Sigma) and L-glutamine (2 mM) (Invitrogen GmbH, Karlsruhe, Germany). The cultures were maintained in an incubator at 37°C and 5% CO2 and were determined to be free of contamination with mycoplasma by PCR assay. Cell line characteristics and culture conditions are further described in supplemental information (Additional file 2: Table S2).

Metaphase spreads and G-Banding

Metaphases were obtained using standardized harvesting protocols for conventional and molecular cytogenetic analysis (M-FISH). Briefly, colcemid solution (0.03 μg/ml) (Sigma) was added to cultures 2.5 hours (h) before cell harvesting; cells were then treated with hypotonic solution, fixed three times with Carnoy's fixative (3:1 methanol to acetic acid) and spread on glass.

Glass slides were baked at 70°C for 24 h, incubated in HCl and placed in 2xSSC buffer before treatment with Wright's stain. Image acquisition and subsequent

karyotyping of metaphases were performed using a Nikon microscope with the cytogenetic software CytoVision System (Applied Imaging, Santa Clara, CA, USA). Chromosome aberrations were described according to the International System for Human Cytogenetic Nomenclature (ISCN) 2013 [36].

Multi-color FISH (M-FISH)

M-FISH was performed with the aim of identifying complex chromosomal rearrangements. The probe cocktail containing 24 differentially labeled chromosome-specific painting probes (24xCyte kit MetaSystems, Altlussheim, Germany) was denatured and hybridized to denatured tumor metaphase chromosomes according to the manufacturer's protocol for the Human Multicolor FISH kit (MetaSystems). Briefly, the slides were incubated at 70°C in saline solution (2xSSC), denatured in NaOH, dehydrated in ethanol series, air-dried, covered with 10 μl of probe cocktail (denatured) and hybridized for two days at 37°C. The slides were then washed with post-hybridization buffers, dehydrated in ethanol series and counter-stained with 10 μl of DAPI/antifade. The signal detection and analysis of subsequent metaphases used the Metafer system and Metasytems' ISIS software (software for spectral karyotypes).

Hierarchical clustering

The first cluster analysis was performed to assess the chromosomal heterogeneity of each cell line by considering the type and frequency of chromosomal alterations within metaphases. Each alteration was computed as present or absent within the karyotype of different metaphases. In the second cluster analysis, the frequency (%) of each chromosomal alteration was compared among the four cell lines. Hierarchical clustering was performed using package gplots from the Bioconductor project (http://www.bioconductor.org) for the R statistical language. A Euclidean distance was used to calculate the matrix of distances, and clusters were built using Ward's method.

Additional files

Additional file 1: Table S1. Upregulated and downregulated genes in HER2+ breast cancer cell lines reported by Wilson, et al. (2002) [35] and located in the chromosomal region observed to be altered in this study and significantly associated with this group.

Additional file 2: Table S2. Characteristics of breast cancer cell lines. Data obtained from ATCC.

Abbreviations

CGH: Comparative genomic hybridization; aCGH: Array comparative genomic hybridization; MLPA: Multiplex ligation dependent probe amplification; ER: Estrogen receptor; M-FISH: Multicolor fluorescence *in situ* hybridization; AC: Adenocarcinoma; IDC: Invasive ductal carcinoma; PE: Pleural effusion; FBS: Fetal bovine serum; DMEM: Dulbecco's modified Eagle's medium.

Competing interests

The authors declare that they have no competing interests.

Authors' contributions

All authors made substantial contributions to conception and design, analysis and interpretation of data, and critical review of the manuscript. AS, MRL, LV and CM conceived the study, coordinated the data acquisition and analysis, and co-wrote the manuscript. MRL, LV, NR, PG and CB coordinated and performed the experiments. MRL, NR and CP performed the biostatistical and hierarchical cluster analysis. SR, GB and BP provided assistance with manuscript preparation. All authors read and approved the final manuscript.

Acknowledgments

This work was supported by AIRC Grants (IG 10787 to AS and MFAG 13310 to CM) and by Ricerca Sanitaria Finalizzata (RF-2010-2310674 to AS). Milena Rondón-Lagos is supported by ERACOL program (Erasmus Mundus External Cooperation Window, EACEA/13/09 - Lot 21b).

Author details

[1]Department of Medical Sciences, University of Turin, Via Santena 7, 10126 Turin, Italy. [2]Department of Laboratory Medicine, Azienda Ospedaliera Città della Salute e della Scienza di Torino, Turin, Italy. [3]Natural and Mathematical Sciences Faculty, Universidad del Rosario, Bogotá, Colombia. [4]Medical Genetics Center, Department of Cell Biology and Genetics, Center of Biomedical Genetics, P.O. Box 1738, 3000 DR Erasmus MC, Rotterdam, The Netherlands.

Received: 23 October 2013 Accepted: 21 January 2014
Published: 23 January 2014

References

1. Kao J, Salari K, Bocanegra M, Choi YL, Girard L, Gandhi J, Kwei KA, Hernandez-Boussard T, Wang P, Gazdar AF, *et al*: **Molecular profiling of breast cancer cell lines defines relevant tumor models and provides a resource for cancer gene discovery.** *PloS One* 2009, **4:**e6146.
2. Kytola S, Rummukainen J, Nordgren A, Karhu R, Farnebo F, Isola J, Larsson C: **Chromosomal alterations in 15 breast cancer cell lines by comparative genomic hybridization and spectral karyotyping.** *Genes Chromosomes Cancer* 2000, **28:**308–317.
3. Lacroix M, Leclercq G: **Relevance of breast cancer cell lines as models for breast tumours: an update.** *Breast Cancer Res Treat* 2004, **83:**249–289.
4. Neve RM, Chin K, Fridlyand J, Yeh J, Baehner FL, Fevr T, Clark L, Bayani N, Coppe JP, Tong F, *et al*: **A collection of breast cancer cell lines for the study of functionally distinct cancer subtypes.** *Cancer Cell* 2006, **10:**515–527.
5. Perou CM, Sorlie T, Eisen MB, van de Rijn M, Jeffrey SS, Rees CA, Pollack JR, Ross DT, Johnsen H, Akslen LA, *et al*: **Molecular portraits of human breast tumours.** *Nature* 2000, **406:**747–752.
6. Sorlie T, Perou CM, Tibshirani R, Aas T, Geisler S, Johnsen H, Hastie T, Eisen MB, van de Rijn M, Jeffrey SS, *et al*: **Gene expression patterns of breast carcinomas distinguish tumor subclasses with clinical implications.** *Proc Natl Acad Sci USA* 2001, **98:**10869–10874.
7. Van 't Veer LJ, Dai H, Van de Vijver MJ, He YD, Hart AA, Mao M, Peterse HL, Van der Kooy K, Marton MJ, Witteveen AT, *et al*: **Gene expression profiling predicts clinical outcome of breast cancer.** *Nature* 2002, **415:**530–536.
8. Goldhirsch A, Wood WC, Coates AS, Gelber RD, Thurlimann B, Senn HJ: **Panel m: Strategies for subtypes–dealing with the diversity of breast cancer: highlights of the St. Gallen International Expert Consensus on the Primary Therapy of Early Breast Cancer 2011.** *Ann Oncol* 2011, **22:**1736–1747.
9. Borgna S, Armellin M, Di Gennaro A, Maestro R, Santarosa M: **Mesenchymal traits are selected along with stem features in breast cancer cells grown as mammospheres.** *Cell Cycle* 2012, **11:**4242–4251.
10. Subik K, Lee JF, Baxter L, Strzepek T, Costello D, Crowley P, Xing L, Hung MC, Bonfiglio T, Hicks DG, Tang P: **The expression patterns of ER, PR, HER2, CK5/6, EGFR, Ki-67 and AR by immunohistochemical analysis in breast cancer cell lines.** *Breast Cancer* 2010, **4:**35–41.
11. Grigoriadis A, Mackay A, Noel E, Wu PJ, Natrajan R, Frankum J, Reis-Filho JS, Tutt A: **Molecular characterisation of cell line models for triple-negative breast cancers.** *BMC Genomics* 2012, **13:**619.

12. Jonsson G, Staaf J, Olsson E, Heidenblad M, Vallon-Christersson J, Osoegawa K, De Jong P, Oredsson S, Ringner M, Hoglund M, Borg A: **High-resolution genomic profiles of breast cancer cell lines assessed by tiling BAC array comparative genomic hybridization.** *Genes Chromosomes Cancer* 2007, **46:**543–558.
13. Shadeo A, Lam WL: **Comprehensive copy number profiles of breast cancer cell model genomes.** *Breast Cancer Res* 2006, **8:**R9.
14. Davidson JM, Gorringe KL, Chin SF, Orsetti B, Besret C, Courtay-Cahen C, Roberts I, Theillet C, Caldas C, Edwards PA: **Molecular cytogenetic analysis of breast cancer cell lines.** *Br J Cancer* 2000, **83:**1309–1317.
15. Gasparini P, Bertolini G, Binda M, Magnifico A, Albano L, Tortoreto M, Pratesi G, Facchinetti F, Abolafio G, Roz L, *et al*: **Molecular cytogenetic characterization of stem-like cancer cells isolated from established cell lines.** *Cancer Lett* 2010, **296:**206–215.
16. Lu YJ, Morris JS, Edwards PA, Shipley J: **Evaluation of 24-color multifluor-fluorescence in-situ hybridization (M-FISH) karyotyping by comparison with reverse chromosome painting of the human breast cancer cell line T-47D.** *Chromosome Res* 2000, **8:**127–132.
17. *The American type culture collection.* www.atcc.org.
18. National Center for Biotechnology Information: *SKY/M-FISH and CGH database.* http://www.ncbi.nlm.nih.gov/projects/sky/skyquery.cgi.
19. Baatout S: **Molecular basis to understand polyploidy.** *Hematol Cell Ther* 1999, **41:**169–170.
20. Dellas A, Torhorst J, Schultheiss E, Mihatsch MJ, Moch H: **DNA sequence losses on chromosomes 11p and 18q are associated with clinical outcome in lymph node-negative ductal breast cancer.** *Clin Cancer Res* 2002, **8:**1210–1216.
21. Gudmundsson J, Barkardottir RB, Eiriksdottir G, Baldursson T, Arason A, Egilsson V, Ingvarsson S: **Loss of heterozygosity at chromosome 11 in breast cancer: association of prognostic factors with genetic alterations.** *Br J Cancer* 1995, **72:**696–701.
22. Karnik P, Paris M, Williams BR, Casey G, Crowe J, Chen P: **Two distinct tumor suppressor loci within chromosome 11p15 implicated in breast cancer progression and metastasis.** *Hum Mol Gen* 1998, **7:**895–903.
23. Winqvist R, Hampton GM, Mannermaa A, Blanco G, Alavaikko M, Kiviniemi H, Taskinen PJ, Evans GA, Wright FA, Newsham I, *et al*: **Loss of heterozygosity for chromosome 11 in primary human breast tumors is associated with poor survival after metastasis.** *Cancer Res* 1995, **55:**2660–2664.
24. Xu XL, Wu LC, Du F, Davis A, Peyton M, Tomizawa Y, Maitra A, Tomlinson G, Gazdar AF, Weissman BE, *et al*: **Inactivation of human SRBC, located within the 11p15.5-p15.4 tumor suppressor region, in breast and lung cancers.** *Cancer Res* 2001, **61:**7943–7949.
25. Marchio C, Lambros MB, Gugliotta P, Di Cantogno LV, Botta C, Pasini B, Tan DS, Mackay A, Fenwick K, Tamber N, *et al*: **Does chromosome 17 centromere copy number predict polysomy in breast cancer? A fluorescence in situ hybridization and microarray-based CGH analysis.** *J Pathol* 2009, **219:**16–24.
26. Sapino A, Goia M, Recupero D, Marchio C: **Current challenges for HER2 testing in diagnostic pathology: state of the art and controversial issues.** *Front Oncol* 2013, **3:**129.
27. Hirata K, Tagawa Y, Kashima K, Kidogawa H, Deguchi M, Tsuji T, Ayabe H: **Frequency of chromosome 7 gain in human breast cancer cells: correlation with the number of metastatic lymph nodes and prognosis.** *Tohoku J Exp Med* 1998, **184:**85–97.
28. Aka JA, Lin SX: **Comparison of functional proteomic analyses of human breast cancer cell lines T47D and MCF7.** *PloS One* 2012, **7:**e31532.
29. Benz CC, Scott GK, Sarup JC, Johnson RM, Tripathy D, Coronado E, Shepard HM, Osborne CK: **Estrogen-dependent, tamoxifen-resistant tumorigenic growth of MCF-7 cells transfected with HER2/neu.** *Breast Cancer Res Treat* 1992, **24:**85–95.
30. Cui J, Germer K, Wu T, Wang J, Luo J, Wang SC, Wang Q, Zhang X: **Cross-talk between HER2 and MED1 regulates tamoxifen resistance of human breast cancer cells.** *Cancer Res* 2012, **72:**5625–5634.
31. Tari AM, Lim SJ, Hung MC, Esteva FJ, Lopez-Berestein G: **Her2/neu induces all-trans retinoic acid (ATRA) resistance in breast cancer cells.** *Oncogene* 2002, **21:**5224–5232.
32. Albertson DG, Collins C, McCormick F, Gray JW: **Chromosome aberrations in solid tumors.** *Nat Gen* 2003, **34:**369–376.
33. Willman CL, RA H: **Genomic alterations and chromosomal aberrations in human cancer.** In *Cancer medicine 7*. London: BC Decker Inc; 2006:104–154.
34. Rajagopalan H, Lengauer C: **Aneuploidy and cancer.** *Nature* 2004, **432:**338–341.
35. Wilson KS, Roberts H, Leek R, Harris AL, Geradts J: **Differential gene expression patterns in HER2/neu-positive and -negative breast cancer cell lines and tissues.** *Am J Pathol* 2002, **161:**1171–1185.
36. ISCN: *An International System for Human Cytogenetic Nomenclature (2013).* Basel, Switzerland: Karger Medical and Scientific Publishers; 2013.

doi:10.1186/1755-8166-7-8
Cite this article as: Rondón-Lagos *et al.*: Differences and homologies of chromosomal alterations within and between breast cancer cell lines: a clustering analysis. *Molecular Cytogenetics* 2014 **7**:8.

BMC Cancer

RESEARCH ARTICLE Open Access

Unraveling the chromosome 17 patterns of FISH in interphase nuclei: an in-depth analysis of the *HER2* amplicon and chromosome 17 centromere by karyotyping, FISH and M-FISH in breast cancer cells

Milena Rondón-Lagos[1,4], Ludovica Verdun Di Cantogno[2], Nelson Rangel[1,4], Teresa Mele[3], Sandra R Ramírez-Clavijo[4], Giorgio Scagliotti[3], Caterina Marchiò[1,2*†] and Anna Sapino[1,2*†]

Abstract

Background: In diagnostic pathology, *HER2* status is determined in interphase nuclei by fluorescence *in situ* hybridization (FISH) with probes for the *HER2* gene and for the chromosome 17 centromere (CEP17). The latter probe is used as a surrogate for chromosome 17 copies, however chromosome 17 (Chr17) is frequently rearranged. The frequency and type of specific structural Chr17 alterations in breast cancer have been studied by using comparative genomic hybridization and spectral karyotyping, but not fully detailed. Actually, balanced chromosome rearrangements (e.g. translocations or inversions) and low frequency mosaicisms are assessable on metaphases using G-banding karyotype and multicolor FISH (M-FISH) only.

Methods: We sought to elucidate the CEP17 and *HER2* FISH patterns of interphase nuclei by evaluating Chr17 rearrangements in metaphases of 9 breast cancer cell lines and a primary culture from a triple negative breast carcinoma by using G-banding, FISH and M-FISH.

Results: Thirty-nine rearranged chromosomes containing a portion of Chr17 were observed. Chromosomes 8 and 11 were the most frequent partners of Chr17 translocations. The lowest frequency of Chr17 abnormalities was observed in the HER2-negative cell lines, while the highest was observed in the HER2-positive SKBR3 cells. The MDA-MB231 triple negative cell line was the sole to show only non-altered copies of Chr17, while the SKBR3, MDA-MB361 and JIMT-1 HER2-positive cells carried no normal Chr17 copies. True polysomy was observed in MDA-MB231 as the only Chr17 alteration. In BT474 cells polysomy was associated to Chr17 structural alterations. By comparing M-FISH and FISH data, in 8 out of 39 rearranged chromosomes only CEP17 signals were detectable, whereas in 14 rearranged chromosomes *HER2* and *STARD3* genes were present without CEP17 signals. *HER2* and *STARD3* always co-localized on the same chromosomes and were always co-amplified, whereas *TOP2A* also mapped to different derivatives and was co-amplified with *HER2* and *STARD3* on SKBR3 cells only.

Conclusion: The high frequency of complex Chr17 abnormalities suggests that the interpretation of FISH results on interphase nuclei using a dual probe assay to assess gene amplification should be performed "with caution", given that CEP17 signals are not always indicative of normal unaltered or rearranged copies of Chr17.

Keywords: Breast cancer, Chromosome 17, Polysomy, CEP17, *HER2*, *TOP2A*, *STARD3*, M-FISH, Chromosomal rearrangements

* Correspondence: caterina.marchio@unito.it; anna.sapino@unito.it
†Equal contributors
[1]Department of Medical Sciences, University of Turin, Via Santena 7, 10126 Turin, Italy
[2]Department of Laboratory Medicine, Azienda Ospedaliera Città della Salute e della Scienza di Torino, Corso Bramante 88, 1026 Tutin, Italy
Full list of author information is available at the end of the article

Background

Chromosome17 (Chr17) is the second most gene-dense chromosome in the human genome [1], containing many genes central to breast cancer development and progression, including oncogenes (*HER2, TOP2A, STARD3, TAU*), tumor suppressor genes *(TP53, BRCA1, HIC-1)* and DNA double-strand break repair genes (*RDM1*) [2-7]. In particular, the *HER2* gene mapping to 17q11-q12 is amplified in 15-20% of all breast cancers [8], it is a prognostic marker for aggressiveness [8] and predicts the response to anti-HER2 agents [8]. An accurate and definitive reporting of *HER2* status is thus essential for appropriate treatment determination. Fluorescence *in situ* hybridization (FISH) with dual probes for *HER2* and for the Chr17 centromere (CEP17) is the technique most frequently used in diagnostic pathology to determine the *HER2* gene status in interphase nuclei. The correction of *HER2* gene copy number using CEP17 signals is required to account for Chr17 polysomy. However, by microarray-based comparative genomic hybridization (CGH) analysis we have recently provided the first direct evidence that true Chr17 polysomy is a rare event in breast cancer [9]. Indeed, a number of CEP17 copies greater than 3 detected by FISH analysis is frequently related to either a gain or amplification of the centromere region, providing another line of evidence that Chr17 usually displays very complex rearrangements.

CGH, loss of heterozygosity (LOH), and molecular genetics studies have shown that Chr17 is rearranged in at least 30% of breast tumors [1,10,11] and presents a number of rearrangement breakpoints mapping to either its short or long arm. In particular, 17p is principally involved in losses, whereas CGH on 17q shows complex combinations of overlapping gains and losses [1,12]. In addition, CGH and spectral karyotyping (SKY) studies have shown that Chr17 is one of the chromosomes most frequently involved in translocations [13]. However the frequency and type of specific structural Chr17 alterations in breast cancer have not been fully detailed. For example, balanced chromosome rearrangements (e.g. translocations or inversions) and low frequency mosaicisms are assessable on metaphases using G-banding karyotype and multicolor fluorescence *in situ* hybridization (M-FISH) only.

The complexity of Chr17 rearrangements calls into question the accuracy of *HER2*/CEP17 ratios evaluated on interphase nuclei for diagnostic purposes. Indeed, unsuspected Chr17 rearrangements may be contributing to the equivocal results following *in situ* hybridization testing, which account for about 10% of all IHC score 2+ carcinomas [14].

The aim of this study was to assess numerical alterations and structural rearrangements of Chr17 in breast cancer cells and to elucidate how these alterations may impact on the *HER2*/CEP17 FISH results on interphase nuclei.

Methods

Cell lines

Nine established breast cancer cell lines [MCF7, T47D, ZR-75-1 (estrogen receptor positive (ER+), *HER2* not amplified), BT474, MDA-MB361 (ER+, *HER2* amplified), SKBR3, JIMT-1 and KPL4 (ER-, *HER2* amplified) and MDA-MB231 (ER-, *HER2* not amplified)] were obtained from the American Type Culture Collection (ATCC, Manassas, USA). The MCF7, T47D, ZR-75-1, SKBR3, JIMT-1 and KPL4 cell lines were cultured in RPMI 1640 medium (Sigma, St. Louis, MO, USA), while the BT474, MDA-MB231 and MDA-MB361 lines were cultured in DMEM medium (Sigma). All culture media were supplemented with 10% fetal bovine serum (FBS) (Sigma), an antibiotic-antimycotic solution (1X) (Sigma) and L-glutamine (2 mM) (Invitrogen GmbH, Karslruhe, Germany). The cultures were maintained in an incubator at 37°C and 5% CO_2.

Tumor samples for primary culture

The study on primary cultures was approved by the ethics institutional review board for "Biobanking and use of human tissue for experimental studies" of the Pathology Units of the Azienda Ospedaliera Città della Salute e della Scienza di Torino. At our Institution, written informed consent is obtained from patients for the use of residual tissues from the diagnostic procedures in research studies.

We analyzed the cells of a triple negative breast carcinoma (TNBC) that metastasized to the peritoneum, giving rise to a peritoneal effusion. The triple negative phenotype was confirmed by immunohistochemistry (IHC) for the estrogen receptor (ER) (Clone SP1, 1:50 diluted, Cell Marque, Rocklin, California), progesterone receptor (PR) (Clone 1A6, 1:50 diluted, Leica Biosystems, Newcastle Upon Tyne, United Kingdom) and by FISH for the *HER2* gene on a cell block obtained after centrifugation of an aliquot of the effusion. The remaining part was used to set up a short-term primary culture according to a protocol recently described [15]. The epithelial origin of the cells was confirmed by the positive expression of cytokeratins (clones AE1/AE3 and PCK26, pre-diluted, Ventana-Diapath, Tucson, AZ, USA) and by the absence of the mesothelial marker calretinin (polyclonal; 1:100 diluted, Invitrogen) using an immunohistochemical procedure on cells grown directly on sterilized slides [15].

G-Banding and karyotyping

Metaphases for performing conventional and molecular cytogenetic analysis (M-FISH and FISH) were obtained

by using standardized harvesting protocols, as recently described [16].

Metaphases image acquisition and subsequent karyotyping were performed by using a Nikon microscope with the cytogenetic software CytoVision System (Applied Imaging, Santa Clara, CA). Between 10 and 26 metaphase cells with good dispersion and morphology were analyzed for each cell line. Chromosome aberrations were described according to the International System for Human Cytogenetic Nomenclature 2013 (ISCN) [17].

Multi-color fluorescence *in situ* hybridization (M-FISH)

M-FISH was performed as recently described [16]. Briefly, we used a probe cocktail containing 24 differentially labeled chromosome-specific painting probes (24xCyte kit MetaSystems, Altlussheim, Germany) that was denatured and hybridized to denatured tumor metaphase chromosomes. The slides were incubated at 70°C in saline solution (2xSSC), denatured in NaOH, dehydrated in an ethanol series, air-dried, covered with 10 μl of the probe cocktail (denatured) and finally hybridized for two days at 37°C. Subsequently, the slides were washed with post-hybridization buffers, dehydrated in an ethanol series and counter-stained with 10 μl of DAPI/antifade. The Metafer system and the Metasytems ISIS software (Carl Zeiss, Metasystems, GmbH) were used for signal detection and metaphase analysis. At least 10 metaphases exhibiting the same derivative chromosomes were studied for each cell line.

FISH for the *HER2, STARD3* and *TOP2A* genes

FISH experiments were performed to define the *HER2, STARD3* (17q12) and *TOP2A* (17q21-q22) gene status and mapping. In *HER2* amplified tumors *STARD3* is included in the smallest region of amplification (SRA) involving *HER2*, whereas *TOP2A* is reported to pertain to a separate amplicon.

Two commercial dual-color probes for *HER2* (SpectrumOrange)/CEP17 (SpectrumGreen) and *TOP2A* (SpectrumOrange)/CEP17 (SpectrumGreen) (all from Abbott Molecular, Downers Grove, IL, USA) were used separately on each cell line.

For the *STARD3* gene, FISH studies were performed using both an alpha satellite probe specific for Chr17 (CEP17) that was directly labeled with a green fluorochrome (Abbott molecular) and a *STARD3* specific locus probe fosmid WI2-2398I17 (17q12) that was made in-house. The clone was obtained from BACPAC Resources Center (Children's Hospital Oakland Research Institute, CA, USA). The UCSC database (http://genome.ucsc.edu, February 2009 release) was queried to localize the probe. The fosmid was expanded, extracted using the QIAGEN Plasmid Purification Kit (QiagenGmbH, Hilden, Germany) and then directly labeled with SpectrumOrange-dUTP

Table 1 Aberrations of Chr17 as revealed by G-Banding, M-FISH and FISH in nine breast cancer cell lines and a primary culture raised from a triple negative breast carcinoma

Cell lines	Type of rearrangement
MCF7 (ER+/HER2-)	der(6)t(6;17;16)(q25;q21;?)[100],der(17)t(8;17)t(1;8)[100],der(17)t(17;19)(p11.1;p12)[65]
T47D (ER+/HER2-)	dic(9;17)t(9;17)(p12;p13)[100]
ZR-75-1 (ER+/HER2-)	der(11)t(11;17)(p15;q?21)[100],der(11)t(11;17)(p15;q?21)t(11;17)(?;q25)[88],der(17)t(6;17)(p12;p11.2)[100]
BT474 (ER+/HER2+)	der(X)t(X;17)(q13;q11q12)del(X)(p21)hsr(17)(q11q12)x2[39],der(11)t(8;17)(q21.1;q11q12)t(11;17)(p15;q11q12)x2[100],der(11)t(11;17)(q?14;q?11.2)hsr(17)(q11q12)[39],der(11)t(11;17)(q?14;?)t(8;17)(?;q?11.2)hsr(17)(q11q12)x2[57],der(13)t(13;17)(q10;q11q12)t(13;17)(q10;q11q12)hsr(17)(q11q12)x2[87],der(17)t(6;17)(?;p13)t(15;17)(q11.2;q25)hsr(17)(q11q12)x2[96]
MDA-MB361 (ER+/HER2+)	der(8)t(8;17)(p21;q11q12)t(5;17)(?;q11q12)hsr(17)(q11q12)[100],der(8)t(8;17)(p21;q25)t(8;17)(q13;q11.2)[100],der(17)t(6;17)(?;q21)[100],der(17)t(7;17)(?;p13)[100], der(17)t(17;20)(p11.1;?)t(9;20)(?;q13.1)t(5;9)(q14;?)[100], der(17)t(17;21)(q21;q22)[100]
SKBR3 (ER-/HER2+)	der(X)t(X;17)(q21;q?21)hsr(17)(q11q12)x2[79], der(17)t(8;17)(q12;?)dup(17)(?)hsr(17)(q11q12)hsr(17)(q21)[100],der(17)t(8;17)(?;q25)dup(17)(q22q25)[37],der(17)t(8;13;14;17;21)(?;q?;q?;q11q12;?)hsr(17)(q11q21)[42],der(17)t(3;8;13;17;17;20)(?;?;q12;q12;?p;?)[74], der(17;17)t(17;17)(q25;?)dup(17)(q22q25)t(17;20)(?;?)[100]
JIMT-1 (ER-/HER2+)	der(3)t(3;12)(p21;?)t(2;3)(?;q12)t(2;17)(?;q11q12)hsr(17)(q11q12)[100], ,der(8)t(8;17)(q13;q11q12)t(8;17)(q11.1;q12)hsr(17)(q11q12)[100],der(17)t(8;17)(?;p13)[67],der(17)t(17;22)(p13;?)t(17;22)(q11.1;?)[100],der(18)t(17;18)(q12;q21)t(16;17)(q23;q12)[100]
KPL4 (ER-/HER2+)	der(1)t(1;17)(p36.3;q11q12)hsr(17)(q11q12)[100],der(6)t(6;17)(p12;q11.2)t(8;17)(q25;?)[93],der(9;13)t(9;17)(p24;q11q12)t(13;17)(p11.2;q11.2)hsr(17)(q11q12)[100], der(17)t(3;17)(q13;q11)t(6;17)(?;q11)[66.6]
MDA-MB231 (ER-/HER2-)	//
TNBC CASE (ER-/HER2-)	der(17)t(8;17)(q21;p12)[100],der(17)t(16;17)(q11.2;q11.1)[15],der(17)del(17)(p11.2)del(17)(q11.2)[69],der(17)t(17;19)(p11.1;?)[15],der(17)t(17;22)(p11.1;q11.2)[62]

The % of cells for which each abnormality was observed is indicated at the end of each abnormality within square brackets. The number of cells examined for chromosome count was 26 for MCF7 cells; 24 for T47D cells; 10 for ZR-75-1 cells and for BT474 cells; 10 for MDA-MB361 cells; 19 for SKBR3 cell; 18 for JIMT-1 cells; 15 for KPL4 cells, 14 for MDA-MB231 cells and 13 for the triple negative breast cancer case (TNBC).

(Abbott Molecular), using the Nick Translation Kit (Abbott Molecular) according to the manufacturer's instructions. The fosmid clone was tested on metaphase and interphase cells of healthy donors, obtained using conventional cytogenetic methods, to analyze the position and strength of the signal, the presence/absence of background and cross-hybridization and the hybridization efficiency.

FISH with the *HER2*/CEP17, *STARD3*/CEP17 and *TOP2A*/CEP17 probes was performed separately on each cell line on fresh slides from methanol and acetic acid fixed cells according to the manufacturers' instructions. Briefly, the slides were washed at 37°C in 2x saline-sodium citrate buffer (SSC), dehydrated in an ethanol series, air-dried, covered with 10 μl of probe, co-denatured in HYBrite System at 70°C for 5 min and hybridized overnight at 37°C. Slides were then washed with a post-hybridization buffer (2xSSC/0.3% Nonidet P-40), dehydrated in an ethanol series and counter-stained with 10 μl DAPI/antifade. Metaphases and nuclei were selected with an AxioImager Z1 epifluorescence microscope (Carl Zeiss, Germany). Analysis of the signal pattern on the interphase nuclei and metaphases was performed with the ISIS software. The number of FISH signals and the localization of the signals were analyzed in at least 10 metaphases and interphase nuclei.

Results

Structural alterations of Chr17

The specific Chr17 alterations we found are detailed in Table 1. In 8 out of the 9 cell lines analyzed we identified 39 rearranged chromosomes containing a portion of Chr17 (mainly its long arm) (Figures 1, 2, 3 and 4). The triple negative MDA-MB231 cells showed no Chr17 alterations, while the *HER2* amplified MDA-MB361, SKBR3 and JIMT-1 cell lines carried no normal copies of Chr17. In particular, the SKBR3 cells harbored 10 different types of structural abnormalities on Chr17, making it the cell

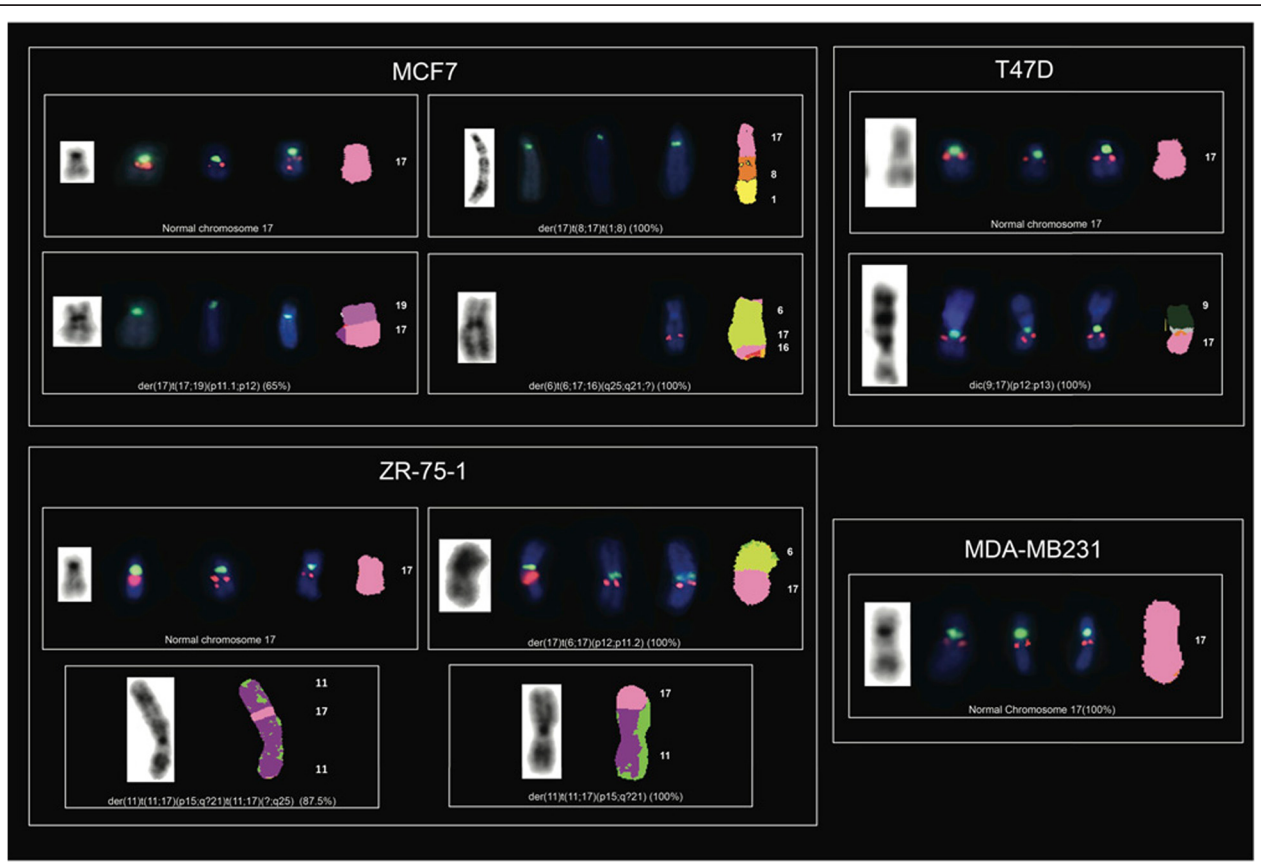

Figure 1 Analysis of Chr17 using G-Banding, dual-color FISH (*HER2*/CEP17, *STARD3*/CEP17 and *TOP2A*/CEP17) and M-FISH in the MCF7, T47D, ZR-75-1 and MDA-MB231 not *HER2* amplified breast cancer cell lines. Rearranged chromosomes containing a portion of Chr17 are visualized by G-Banding technique on the left and by M-FISH on the right. For M-FISH the classified color of Chr17 is shown in pink, the translocation partners are numbered on the right hand side of the chromosomes and the frequency at which each abnormality was observed is indicated in brackets at the end of each abnormality. CEP17, *HER2, STARD3* and *TOP2A* are shown in the middle by dual-color FISH (*HER2*/CEP17, *STARD3*/CEP17, *TOP2A*/CEP17, respectively) whenever mapped to the corresponding derivatives (CEP17 is green-labeled; *HER2, STARD3* and *TOP2A* genes are red-labeled).

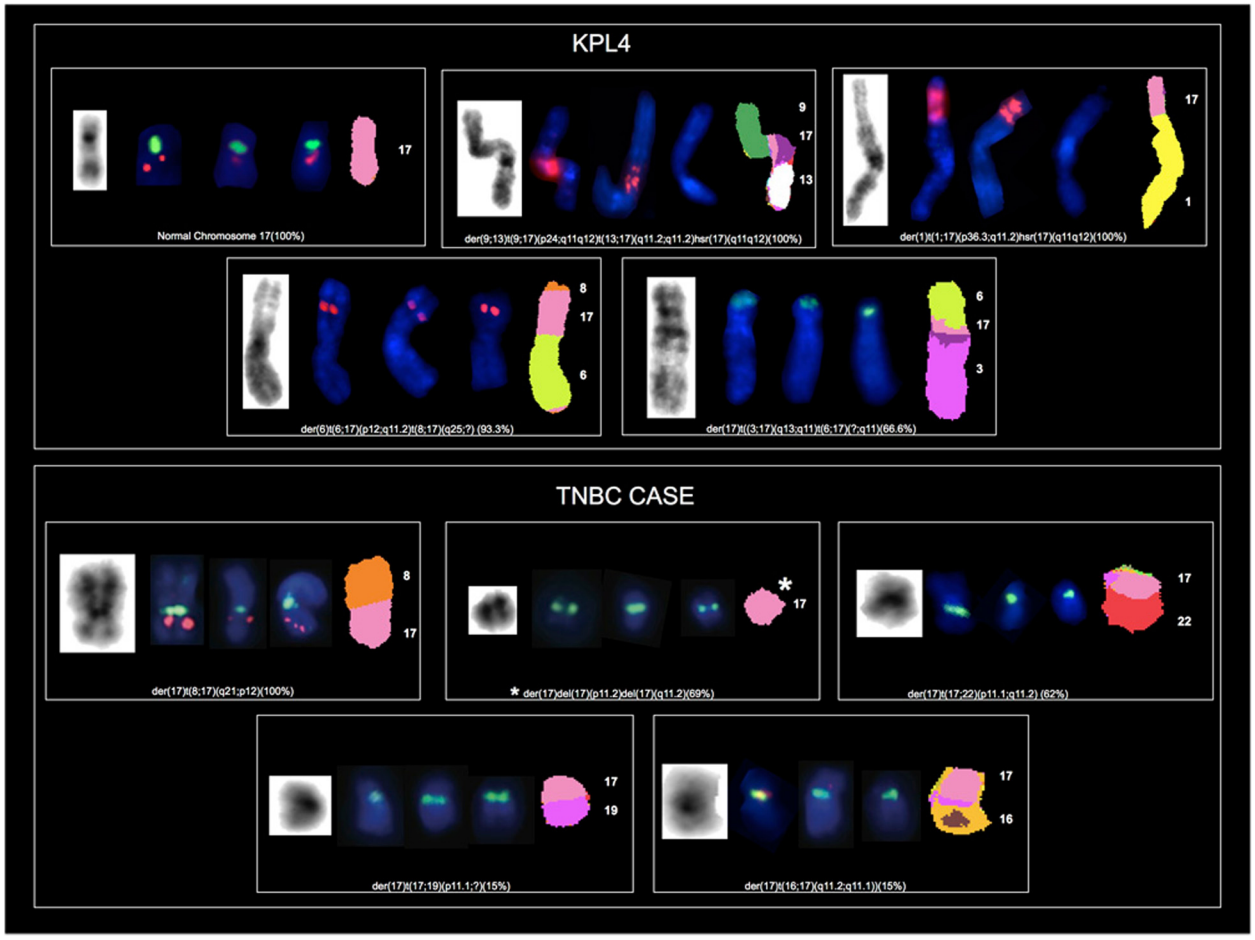

Figure 2 Analysis of Chr17 using G-Banding, dual-color FISH (*HER2*/CEP17, *STARD3*/CEP17 and *TOP2A*/CEP17) and M-FISH in KPL4 *HER2* amplified breast cancer cell line showing four translocated Chr17 in addition to the normal-appearing copies of Chr17 and in one triple negative breast cancer case (TNBC) showing five rearranged copies of Chr17. Rearranged chromosomes containing a portion of Chr17 are visualized by G-Banding technique on the left and by M-FISH on the right. For M-FISH the classified color of Chr17 is shown in pink, the translocation partners are numbered on the right hand side of the chromosomes and the frequency at which each abnormality was observed is indicated in brackets at the end of each abnormality. CEP17, *HER2, STARD3* and *TOP2A* are shown in the middle by dual-color FISH (*HER2*/CEP17, *STARD3*/CEP17, *TOP2A*/CEP17, respectively) whenever mapped to the corresponding derivatives (CEP17 is green-labeled; *HER2, STARD3* and *TOP2A* genes are red-labeled). In the TNBC cells the chromosome in which we identified Chr17 material only is a der(17)del(17)(p11.2)del(17)(q11.2) with a deletion on both short and long arm involving 17q12-q21.

line with the highest frequency of structural abnormalities. The lowest frequency of Chr17 abnormalities was observed in HER2 negative cells, which carried between 2 and 3 different types of alterations.

We defined nine regions of Chr17 frequently involved in the observed structural alterations: 17p11, 17p13, 17q11.2, 17q11-12, 17q12, 17q21, 17q22, 17q23 and 17q25. The 17q11-12 region was the most frequent long arm portion involved in structural alterations. This region was affected in the BT474, MDA-MB361, SKBR3, JIMT-1 and KPL4 *HER2* amplified cell lines, while 17p11 and 17p13 were commonly affected in the MCF7, ZR-75-1, MDA-MB361 and the SKBR3 and in T47D, MDA-MB361, JIMT-1 cells, respectively (Table 1).

Using G-Banding, numerous complex derivative chromosomes containing material from Chr17 were observed in all cell lines except for MDA-MB231. Some of the derivative chromosomes were present in duplicate (Table 1). Chr17 deletions and dicentric chromosomes were observed only in the T47D and SKBR3 cells.

M-FISH demonstrated that chromosome 8 and chromosome 11 were the most frequent translocation partners of Chr17 (Table 2). Twelve different rearrangements between Chr17 and chromosome 8, involving mainly their long arms (8q11.1, 8q12, 8q13, 8q21 and 8q24) were identified in MCF7, MDA-MB361, BT474, SKBR3 and JIMT-1 cells. Similarly, 5 translocations between Chr17 (long arm) and chromosome 11 (involving 11p15, 11q13 and 11q23) were

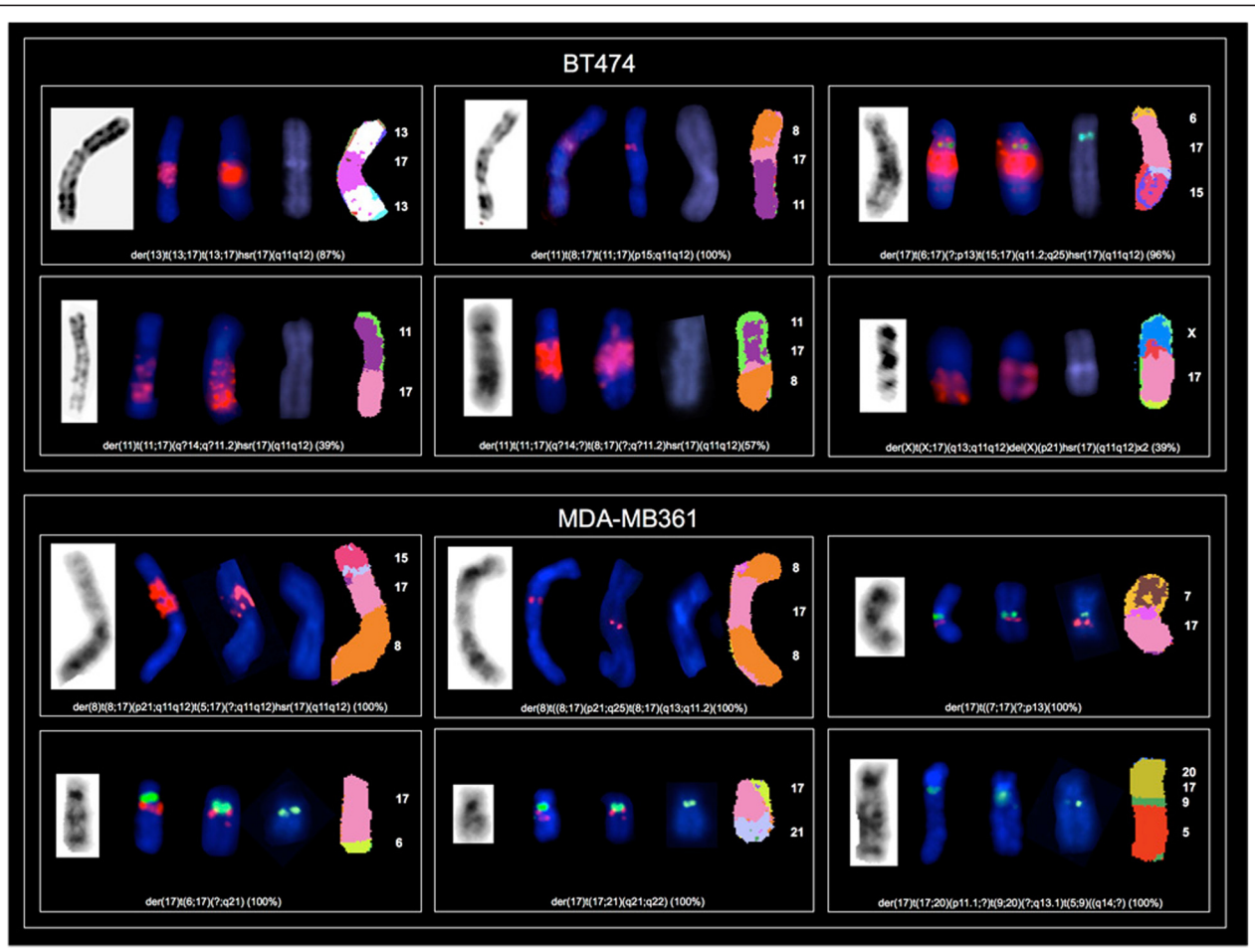

Figure 3 Analysis of Chr17 using G-Banding, dual-color FISH (*HER2*/CEP17, *STARD3*/CEP17 and *TOP2A*/CEP17) and M-FISH in BT474 and MDA-MB361 *HER2* amplified breast cancer cell lines showing six translocated copies of Chr17. Rearranged chromosomes containing a portion of Chr17 are visualized by G-Banding technique on the left and by M-FISH on the right. For M-FISH the classified color of Chr17 is shown in pink, the translocation partners are numbered on the right hand side of the chromosomes and the frequency at which each abnormality was observed is indicated in brackets at the end of each abnormality. CEP17, *HER2, STARD3* and *TOP2A* are shown in the middle by dual-color FISH (*HER2*/CEP17, *STARD3*/CEP17, *TOP2A*/CEP17, respectively) whenever mapped to the corresponding derivatives (CEP17 is green-labeled; *HER2, STARD3* and *TOP2A* genes are red-labeled).

identified in ZR-75-1 and BT474 cells. Translocations with chromosome 6 were observed in five cell lines, and translocations between Chr17 and chromosomes X, 1, 3, 7 and 16 were observed only in HER2 positive cells (Table 2). We identified 5 different alterations of Chr17 in the primary TNBC culture, involving both the short (17p11.1, 17p11.2, 17p12) and the long (17q11.1 and 17q11.2) arms. In addition, numerous complex Chr17 derivatives containing material from chromosomes 8, 16, 19 and 22 were observed.

Mapping CEP17 and the 17q12–q21 amplicon

We considered the chromosomal correlation of *HER2, STARD3* and *TOP2A* genes mapping to 17q12–q21 with CEP17 as shown by FISH on metaphase chromosomes and we compared the results to the interphase pattern. By M-FISH we reported the specific rearrangements. Out of the 39 rearranged chromosomes containing a portion of Chr17 identified by M-FISH, 12 harbored *HER2*, *STARD3* (which mapped always together) and *TOP2A*; 16 harbored *HER2* and *STARD3*, 1 harbored only *TOP2A*, 2 did not show either CEP17, *HER2*, *STARD3* or *TOP2A* signals.

Notably, 8 of the 39 rearranged chromosomes carried CEP17 signals without *HER2* and *STARD3* signals and 14 harbored *HER2* and *STARD3* genes but not CEP17.

The specific patterns observed by FISH in each cell line are reported below.

Triple negative cell lines

In the MDA-MB231 triple negative cells the FISH (both in interphase and metaphase) and M-FISH patterns corresponded to three copies of normal Chr17, each with one CEP17 green signal and one red signal

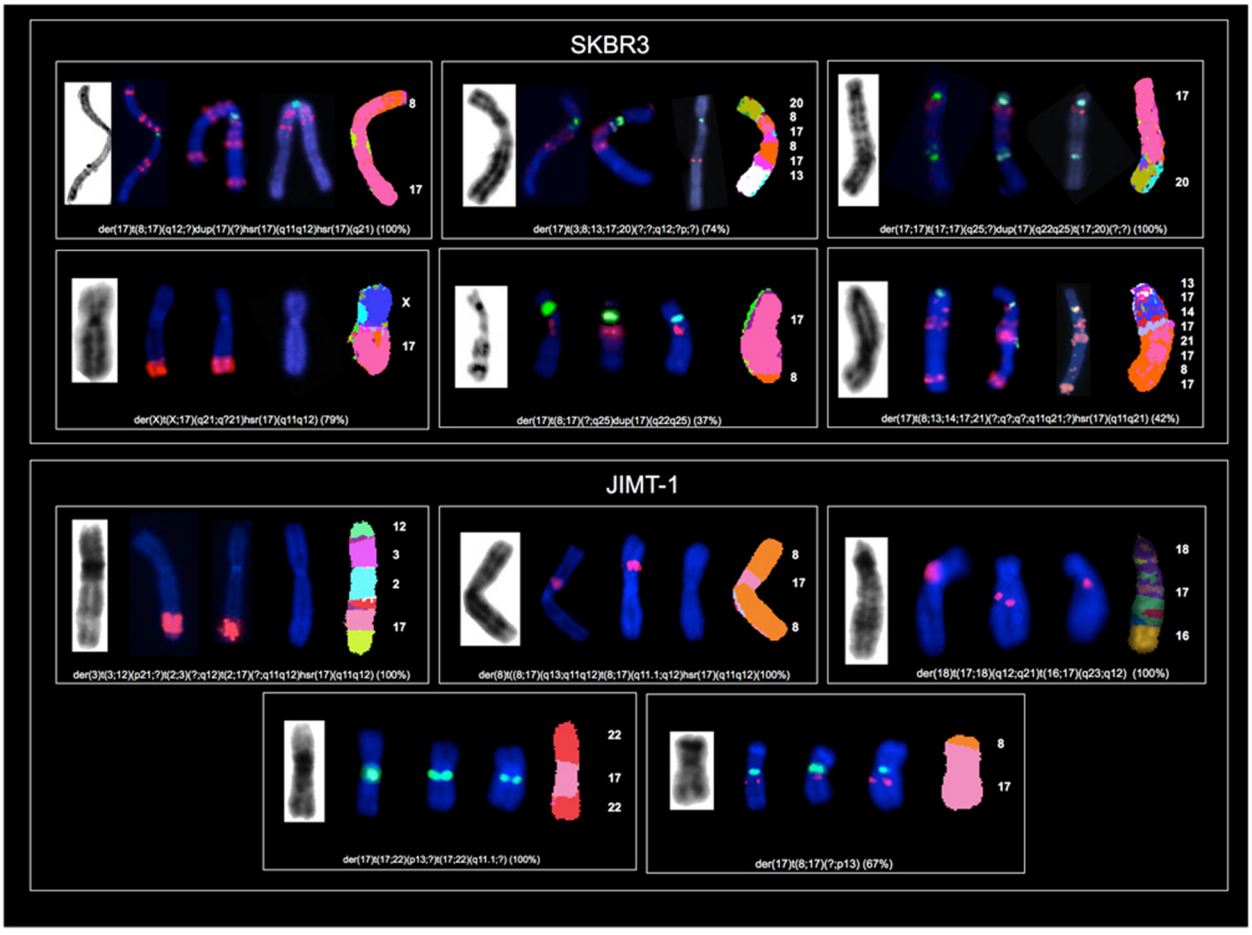

Figure 4 Analysis of Chr17 using G-Banding, dual-color FISH (*HER2*/CEP17, *STARD3*/CEP17 and *TOP2A*/CEP17) and M-FISH in SKBR3 and JIMT-1 *HER2* amplified breast cancer cell lines showing four or six translocated copies of Chr17. Rearranged chromosomes containing a portion of Chr17 are visualized by G-Banding technique on the left and by M-FISH on the right. For M-FISH the classified color of Chr17 is shown in pink, the translocation partners are numbered on the right hand side of the chromosomes and the frequency at which each abnormality was observed is indicated in brackets at the end of each abnormality. CEP17, *HER2, STARD3* and *TOP2A* are shown in the middle by dual-color FISH (*HER2*/CEP17, *STARD3*/CEP17, *TOP2A*/CEP17, respectively) whenever mapped to the corresponding derivatives (CEP17 is green-labeled; *HER2, STARD3* and *TOP2A* genes are red-labeled).

corresponding to either *HER2, STARD3* or *TOP2A* (Table 3, Figures 5 and 1).

The TNBC primary culture nuclei displayed the same FISH pattern for the *HER2, STARD3*, *TOP2A* genes and CEP17. Four green CEP17 signals and two red signals were observed (Figures 5 and 2). Two red and two green signals corresponded to two Chr17 derivatives, namely der(17)t(8;17)(q21;p12)x2 (100%), while the other two green signals (without the *HER2, STARD3* and *TOP2A* genes) mapped to der(17)t(17;22)(p11.1;q11.2) (62%) and der(17)del(17)(p11.2)del(17)(q11.2) (69%). This last Chr17 derivative showed deletion on both short and long arms involving the 17q12-21 region (Figure 2).

ER+/HER2 not amplified cell lines

In T47D and ZR-75-1 interphase nuclei, the same copy numbers of *HER2, STARD3* and *TOP2A* genes and of CEP17 were observed (Table 3, Figure 5). Four copies were observed in the T47D nuclei and three in the ZR-75-1 nuclei (Table 3, Figure 5).

The T47D cells showed two normal Chr17 and two Chr17 derivatives carrying both CEP17 and the three genes (Figures 5 and 1). M-FISH showed that the derivative chromosome previously reported as der(9)t(9;17)(p13;q11) [18] was a dic(9;17)t(9;17)(p12;p13) (Figure 1).

In ZR-75-1, M-FISH showed that *HER2, STARD3* and *TOP2A* genes mapped to two normal Chr17 and one derivative Chr17 (Table 3, Figures 5 and 1).

MCF7 interphase nuclei displayed four CEP17 green signals and two red signals for the *HER2* and *STARD3* genes (Table 3, Figure 6). This pattern corresponded to one CEP17 signal and one copy of the *HER2* and *STARD3* genes located on two normal Chr17 and two CEP17 signals on two Chr17 derivatives as confirmed by M-FISH

Table 2 Frequency of translocation partners of Chr17 in nine breast cancer cell lines

Translocation partner	Chromosomal abnormality	Number of abnormalities	No of cell lines	Cell lines
Chromosome 8	der	12	5	MCF7, MDA-MB361, SKBR3, JIMT-1, BT474
Chromosome 11	der	5	2	ZR-75-1, BT474
Chromosome 6	der	5	5	MCF7, ZR-75-1, MDA-MB361, BT474, KPL4
Chromosome X	der	2	2	BT474, SKBR3
Chromosome 9	der	2	2	KPL4, T47D
Chromosome 9	dic	1	1	T47D
Chromosome 3	der	2	2	JIMT-1, KPL4
Chromosome 7	der	1	1	MDA-MB361
Chromosome 13	der	2	2	BT474, KPL4
Chromosome 1	der	1	1	KPL4
Chromosome 16	der	1	1	JIMT-1
Chromosome 17	der	1	1	SKBR3
Chromosome 19	der	1	1	MCF7
Chromosome 20	der	1	1	MDA-MB361
Chromosome 21	der	1	1	MDA-MB361
Chromosome 22	der	1	1	JIMT-1

der = derivative chromosome; dic = dicentric chromosome.

(Figure 1). The FISH pattern for *TOP2A* was similar to that observed for the *HER2* and *STARD3* genes, with the only exception of having an additional *TOP2A* copy mapping on a derivative chromosome 6 (Figures 6 and 1).

HER2 amplified cell lines

HER2, TOP2A and *STARD3* gene amplifications were found within chromosomes as homogeneously staining regions (HSRs) but not in extra-chromosomal, double-minute chromosomes (DMs). All of these cell lines showed *HER2* and *STARD3* co-amplification.

In BT474 interphase nuclei, six CEP17 signals and several clusters of *HER2* and *STARD3* were observed. This pattern corresponded to nine clusters and six individual red signals in metaphases (Figure 6). By comparing FISH and M-FISH data, we showed that four CEP17 and four red signals were located on four normal copies of Chr17, and two CEP17 signals and two clusters of red signals on two Chr17 derivatives as shown by M-FISH: der(17)t(6;17)(?;p13)t(15;17)(q11.2;q25)hsr(17)(q11q12)x2 (96%). The remaining seven clusters of red signals mapped to five previously unreported highly rearranged chromosomes (Table 3, Figure 3).

BT474 cells showed normal *TOP2A* gene copy numbers, and four red signals were observed on four normal copies of Chr17 only (Figures 6 and 3).

In the MDA-MB361 nuclei four CEP17 signals, one red cluster and four individual red signals (*HER2* and *STARD3*) were observed (Figure 6). None of these green and red signals were located on normal copies of Chr17 (Table 3, Figure 3). Three individual red signals were correlated with the centromeric locus and located on three Chr17 derivatives. The other individual red signal mapped to a chromosome 8 derivative and the only red cluster, indicative of *HER2* and *STARD3* amplification, was located on another chromosome 8 derivative. The remaining CEP17 signals, without red signal (*HER2* and *STARD3* deletion), mapped to a complex translocation of Chr17 involving chromosomes 5, 9 and 20 (Figure 3).

These cells harbored a *TOP2A* deletion, as four chromosomes with CEP17 were identified, but only one of them had a *TOP2A* signal (Figures 6 and 3).

In the SKBR3 cells, *HER2* and *STARD3* co-amplification was observed in 100% of metaphase and interphase nuclei analyzed. Seven CEP17 signals and sixteen clusters and four individual red signals (*HER2* and *STARD3*) were observed on numerous highly rearranged chromosomes (Table 3 and Figure 6). In particular, two CEP17 and one red signal mapped to the dicentric Chr17, der(17;17)t(17;17)(q25;?)dup(17)(q22q25)t(17;20)(?;?) (100%), which had not been previously reported (Figure 4). In two Chr17 derivatives *TOP2A* was co-amplified with *HER2* either as a single amplicon (der(17)t(8;13;14;17;21)(?;q?;q?;q11q12;?)hsr(17)(q11q21)) or as separate amplicons (der(17)t(8;17)(q12;?)dup(17)(?)hsr(17)(q11q12)hsr(17)(q21)) (Figure 4). In addition, *TOP2A* deletion was detected on der(X)t(X;17)(q21;q?21)hsr(17)(q11q12). In the remaining derivative chromosomes without gene amplification, *TOP2A* showed the same FISH pattern observed for *HER2*, in

Table 3 *HER2* and *STARD3* FISH pattern and complex Chr17 rearrangements in nine breast cancer cell lines and one primary culture raised from a triple negative breast carcinoma

Cell line	CEP 17 signals (green)	*HER2* signals (red)		Chr17		Complex abnormalities encompassing *HER2* Amplification
		Cluster	Individual	Normal	Derivatives	
MCF7	4	0	2	2*	der(17)t(8;17)t(1;8)	
					der(17)t(17;19)(p11.1;p12)	
T47D	4	0	4	2*	dic(9;17)(p12;p13)*x2	
ZR-75-1	3	0	3	2*	der(17)t(6;17)(p12;p11.2)*	
BT474	6	9	6	4*	der(17)t(6;17)(?;p13)t(15;17)(q11.2;q25)hsr(17)(q11q12**)x2	der(X)t(X;17)(q13;q11q12)del(X)(p21)hsr(17)(q11q12**)x2
						der(11)t(8;17)(q21.1;q11q12*)t(11;17)(p15;q11q12)x2
						der(11)t(11;17)(q?14;q?11.2)hsr(17)(q11q12**)
						der(11)t(11;17)(q?14;?)t(8;17)(?;q?11.2)hsr(17)(q11q12**)x2
						der(13)t(13;17)(q10;q11q12)t(13;17)(q10;q11q12)hsr(17)(q11q12**)x2
						der(17)t(6;17)(?;p13)t(15;17)(q11.2;q25)hsr(17)(q11q12**)x2
MDA-MB361	4	1	4	0	der(17)t(6;17)(?;q21)*	der(8)t(8;17)(p21;q11q12)t(5;17)(?;q11q12)hsr(17)(q11q12**)
					der(17)t(7;17)(?;p13)*	der(8)t(8;17)(p21;q25)t(8;17)(q13;q11.2*)
					der(17)t(17;20)(p11.1;?)t(9;20)(?;q13.1)t(5;9)(q14;?)	
					der(17)t(17;21)(q21;q22)*	
SKBR3	7	16	4	0	der(17)t(8;17)(q12;?)dup(17)(?)hsr(17)(q11q12**/**/**/**/**/**)hsr(17)(q21)x2	der(X)t(X;17)(q21;q?21)hsr(17)(q11q12**)x2
					der(17)t(8;17)(?;q25)dup(17)(q22q25)*	der(17)t(8;17)(q12;?)dup(17)(?)hsr(17)(q11q12**/**/**/**/**/**)hsr(17)(q21)x2
					der(17)t(8;13;14;17;21)(?;q?;q?;q11q12;?) hsr(17)(q11q21**/**)	der(17)t(8;13;14;17;21)(?;q?;q?;q11q12;?)hsr(17)(q11q21**/**)
					der(17)t(3;8;13;17;17;20)(?;?;q12*;q12*;?p;?)	
					der(17;17)t(17;17)(q25;?)dup(17)(q22q25)t(17;20)(?;?)*	
JIMT-1	2	2	2	0	der(17)t(8;17)(?;p13)*	der(3)t(3;12)(p21;?)t(2;3)(?;q12)t(2;17)(?;q11q12)hsr(17)(q11q12**)
					der(17)t(17;22)(p13;?)t(17;22)(q11.1;?)	der(8)t(8;17)(q13;q11q12)t(8;17)(q11.1;q12)hsr(17)(q11q12**)
KPL4	3	2	3	2*	der(6)t(6;17)(p12;q11.2*)t(8;17)(q25;?)	der(1)t(1;17)(p36.3;q11q12)hsr(17)(q11q12**)
					der(17)t(3;17)(q13;q11)t(6;17)(?;q11)	der(9;13)t(9;17)(p24;q11q12)t(13;17)(p11.2;q11.2)hsr(17)(q11q12**)
MDA-MB231	3	0	3	3*	0	0
TNBC CASE	4	0	2	0	der(17)t(8;17)(q21;p12)*x2	
					der(17)del(17)(p11.2)del(17)(q11.2)	
					der(17)t(17;22)(p11.1;q11.2)	

*Indicates the presence of one red signal (*HER2*) on a normal Chr17 or on a derivative Chr17.
**Indicates the presence of one red cluster (*HER2*) on a derivative Chr17.
/Indicates the presence of two red clusters (*HER2*) on a derivative Chr17.
//**/**/**/**Indicates the presence of six red clusters (*HER2*) on a derivative Chr17.
Scoring of interphase nuclei to obtain the final result on *HER2* gene status performed based both on a dual-FISH and a single FISH assay (according o the new ASCO/CAP guidelines [19]) showed no differences in the final result for each of the cell lines.

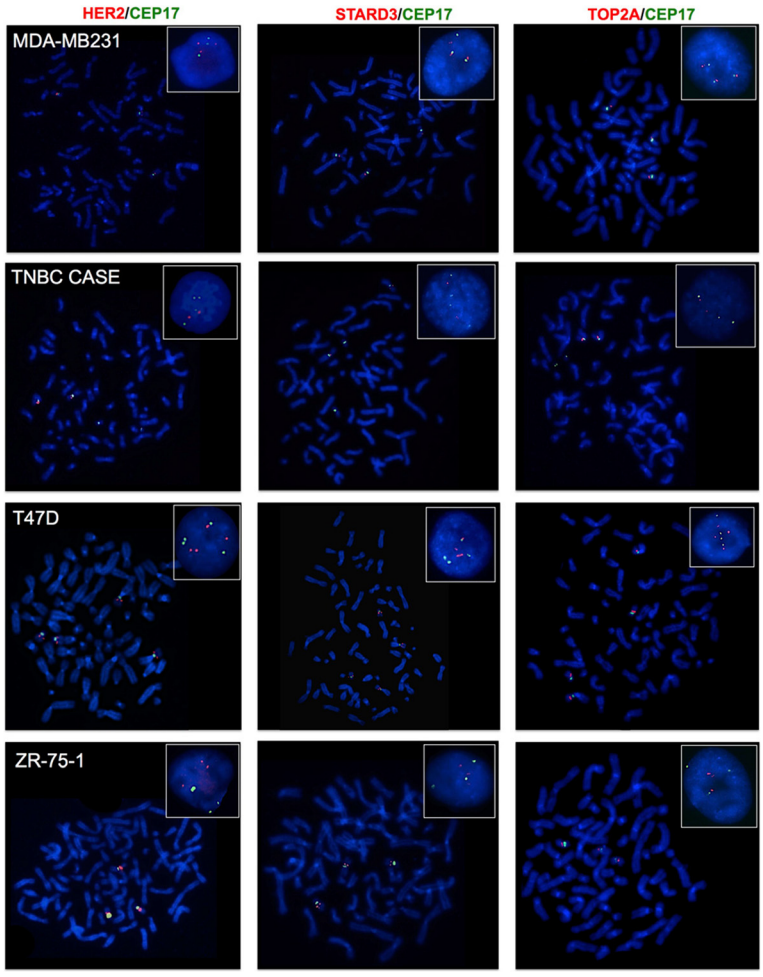

Figure 5 Representative FISH images of the MDA-MB231, T47D and ZR-75-1 breast cancer cells and one TNBC case using *HER2*/CEP17, *STARD3*/CEP17 and *TOP2A*/CEP17 dual-color probes. Metaphase spreads are shown and boxes indicate representative interphase nuclei for each case. None of these cell lines showed amplification of the *HER2, STARD3* or *TOP2A* genes. Gene signals are red-labeled, CEP17 signals are green-labeled.

which all distinct *HER2* genes were accompanied by distinct *TOP2A* genes (Figures 4 and 6).

In the JIMT-1 cells, two CEP 17 signals and two clusters and two individual red signals were observed for *HER2* and *STARD3* genes (Figure 7). The two clusters of red signals mapped to two chromosomes lacking CEP17 (Table 3 and Figure 4). One of the two individual red signals was observed on a Chr17 derivative while the other was on a chromosome 18 derivative (Table 3 and Figure 4). We also observed *HER2* and *STARD3* deletion on der(17)t(17;22)(p13;?)t(17;22)(q11.1;?) (Figure 4).

TOP2A was not amplified and the FISH pattern showed two red and two CEP17 signals: one red signal mapped to a Chr17 derivative, while the other mapped to a chromosome 18 derivative. In addition, a loss of the *TOP2A* gene (*TOP2A* deletion) was observed on der(17)t(17;22)(p13;?)t(17;22)(q11.1;?), similar to that observed for the *HER2* and *STARD3* genes (Figure 4). *TOP2A* signals were not observed on derivative chromosomes with *HER2* amplification (Figure 4).

The KPL4 cells showed three CEP17 signals and two clusters and three individual red signals of *HER2* and *STARD3* genes (Figure 7). Two CEP17 and two red signals were located on two normal copies of Chr17, the other green and red individual signals corresponded to complex rearrangements involving Chr17 (Table 3, Figure 2). Like the JIMT-1 cells, the *HER2* and *STARD3* gene clusters were located on highly rearranged chromosomes (Table 3, Figure 2).

These cells did not show *TOP2A* gene amplification (Figure 7). Instead, one CEP17 signal and one red signal were observed each on two distinct normal Chr17 copies, and one red signal mapped to a chromosome 6 derivative (Figure 2).

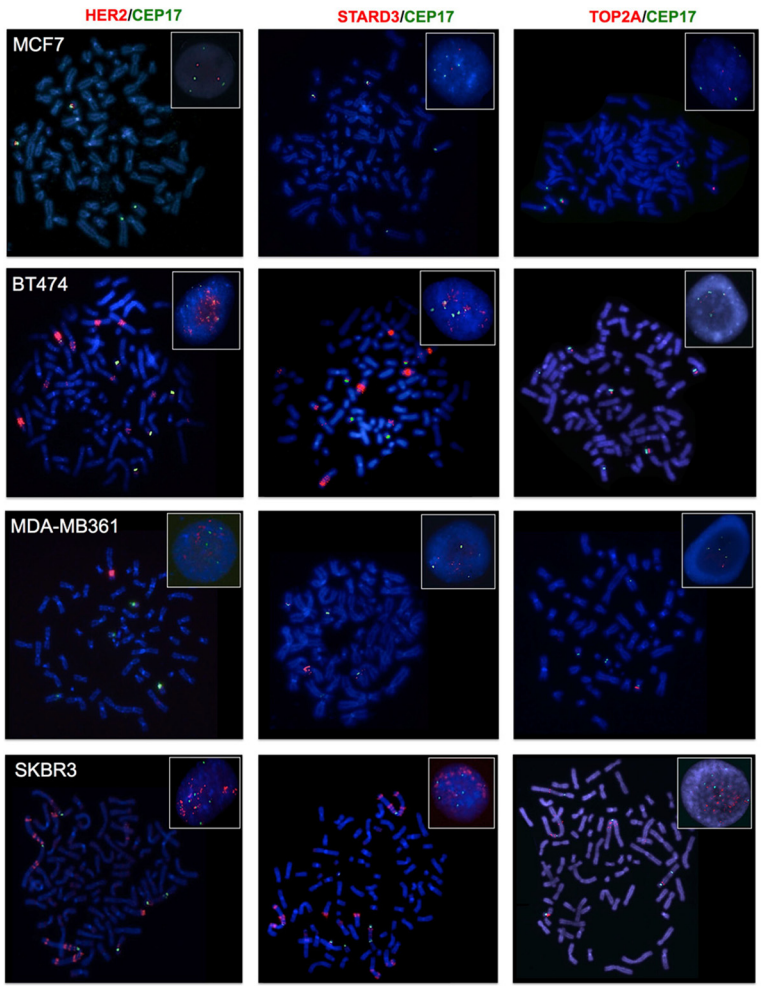

Figure 6 Representative FISH images of the MCF7, BT474, MDA-MB361 and SKBR3 breast cancer cell lines using *HER2*/CEP17, *STARD3*/CEP17 and *TOP2A*/CEP17 dual-color probes. Metaphase spreads are shown and boxes indicate representative interphase nuclei for each case. FISH images for the BT474, MDA-MB361 and SKBR3 cells demonstrated *HER2* and *STARD3* gene amplification, while *TOP2A* gene amplification was observed in the SKBR3 cells only. Gene signals are red-labeled, CEP17 signals are green-labeled.

Discussion

By comparing the *HER2*/CEP17 FISH pattern in metaphase *versus* interphase nuclei, the present study demonstrated that a CEP17 signal rarely corresponds to a single intact Chr17, in both HER2+ and HER2- cell lines. It is well known that cells of long-term cultures may show high chromosomal rearrangements, however Chr17 was altered even in the short-term TNBC primary culture. Although obtained in a single primary cell line this specific finding may corroborate our hypothesis that chromosomal alterations involving Chr17 in breast cancer may be indeed very complex and merit further investigation in primary cell cultures obtained from carcinomas of different phenotypes.

This extensive cytogenetic analysis of Chr17 demonstrated that only the MDA-MB231 triple negative showed true polysomy (normal chromosome acquisition) as the only Chr17 alteration. The BT474 HER2-positive cells showed Chr17 polysomy together with different Chr17 rearrangements. In ER+/*HER2* not amplified cell lines normal copies of Chr17 coexist with rearranged Chr17 copies that either harbor or do not harbor the *HER2* gene. On the other hand, some of the *HER2* amplified cell lines did not show any normal copies of Chr17 and the *HER2-STARD3* gene clusters were observed as HSR on complex rearranged chromosomes. In addition, the Chr17 derivatives (carrying CEP17) did not always show *HER2* gene clusters, and these latter were not exclusively observed in Chr17 derivatives. In particular, in the BT474 cells 7 of 9 *HER2* gene clusters were found on derivatives lacking CEP17.

In breast cancer specimens the analysis of the *HER2* gene in interphase nuclei is requested after an equivocal immunohistochemical result (score 2+) of HER2 expression

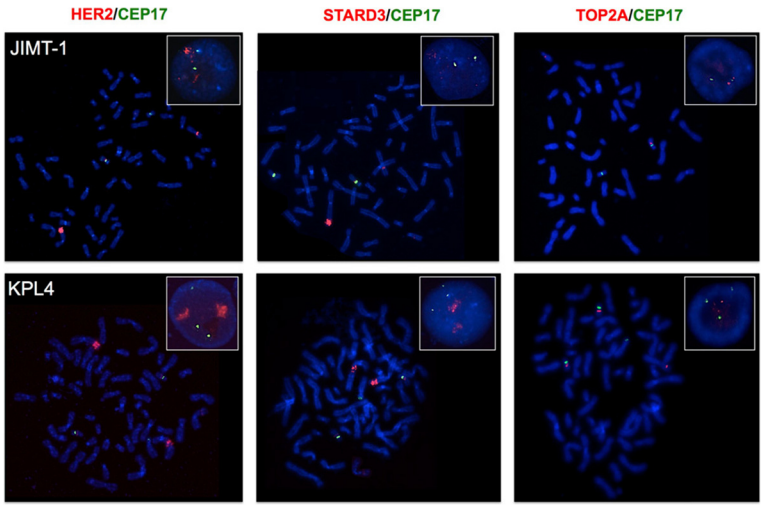

Figure 7 Representative FISH images of the JIMT-1 and KPL4 breast cancer cell lines using *HER2*/CEP17, *STARD3*/CEP17 and *TOP2A*/CEP17 dual-color probes. Metaphase spreads are shown and boxes indicate representative interphase nuclei for each case. FISH images for the JIMT-1 and KPL4 cells demonstrate *HER2* and *STARD3* gene amplification, while *TOP2A* gene amplification was not observed in these cells. Gene signals are red-labeled, CEP17 signals are green-labeled.

[8,19]. Either double-signal (*HER2* and CEP17 probes) or single-signal (*HER2* probe) assays may be performed assessing the *HER2*/CEP17 ratio or the absolute *HER2* copy number, respectively. In the case of the double-signal assay, the recent ASCO/CAP guidelines [19] recommend using the *HER2*/CEP17 ratio to screen for amplified or not amplified breast cancers. However, our data provide another line of evidence that the interpretation of the results of the ISH analyses on interphase nuclei using a dual-signal assay should be performed "with caution", given the high frequency of complex Chr17 abnormalities involving both CEP17 and *HER2* loci. This has to be taken particularly into account in cases showing an increased number of discrete *HER2* signals, in which the *HER2*/CEP17 ratio may highly impact on the final definition of the gene status, in contrast with cases with *HER2* gene clusters of amplification. The introduction by the ASCO/CAP 2013 of an algorithm that takes into account the ratio first and then the *HER2* gene copy numbers represents an improvement in the identification of HER2 positive tumors by dual-signal assays. We should point out that the sole *HER2* gene copy number method, as used in single-signal assay, best identifies *HER2* gene amplification in interphase nuclei, as CEP17 copy numbers do not reflect Chr17 copy numbers. This finding should be taken particularly into account for those scenarios in which monosomy of Chr17 may be encountered. In this respect the new guidelines seem to be controversial depending on the method of ISH analysis employed. Indeed, by following the single signal copy number method cases with low copy number (<4) are labeled as negative, while the same tumors showing monosomy of Chr17 are labeled as positive if the *HER2*/CEP17 ratio is employed [19-21]. Although on one side the *HER2*/CEP17 ratio may still lead to issues when interpreting Chr17 monosomy and *HER2* copy numbers would be more reliable, on the other hand we should also acknowledge that double signal assays with CEP17 counts may still provide informative parameters. Interestingly, a recent study on patients treated with anthracycline-based chemotherapy in the neoadjuvant setting has shown that CEP17 duplication strongly correlated with higher pCR rates [22] than did *TOP2A* and *HER2*, in both univariable and multivariable analyses. This shows that alteration of CEP17 copy number detectable in interphase nuclei may still represent a prognostic or predictive indicator, although we cannot decipher the real complexity of the rearrangements this chromosome undergoes to. For instance, Chr17 was frequently translocated with chromosome 8 and 11. These chromosomes have been observed in translocations in many breast cancer cell lines [13,23] and have also been shown to participate in translocation events in cases of primary breast carcinomas [24]. Cytogenetic analysis of primary cultures would be of invaluable help in understanding whether such alterations recapitulate those of primary tumors. In the primary culture here analyzed, chromosome 8 was involved in one of the translocations.

Another finding of our analyses is the invariable co-amplification of *HER2* and *STARD3* on the same metaphase chromosomes. Increased co-amplification of *HER2* and *STARD3* has been described to be correlated with acquired lapatinib resistance [23]. On the other hand, the simultaneous amplification of *HER2* and *TOP2A* was only found in SKBR3 cells, where a pattern of amplification

distinct from *HER2* was identified in one of the Chr17 derivatives. This observation provides another line of evidence that, despite the genomic proximity of *HER2* and *TOP2A* and the observation that *TOP2A* amplification seems to be restricted to tumors harboring *HER2* amplification, these two genes are likely to pertain to separate amplicons, as previously suggested [24,25]. One may speculate that secondary rearrangements may intervene to separate the two genes from the primary amplicons.

Conclusion

The results of the traditional karyotyping and of FISH and M-FISH assays on metaphase nuclei reported in this study highlight that complex structural alterations of Chr17 encompassing the *HER2* gene and CEP17 are common in breast cancer cell lines. This may reflect the scenario found in breast carcinomas, as this finding was also observed in the primary cell culture raised from a TNBC. Taken together these data indicate that the *HER2*/CEP17 ratio of interphase nuclei, routinely used to select patients for eligibility for anti-HER2 treatment, should be considered with caution and always coupled with the *HER2* gene copy number values in order not to misinterpret *HER2* gene amplification, as recently updated in the ASCO/CAP 2013 [19].

Further investigation on primary cell cultures would be of invaluable help to allow functional analysis in cells harboring Chr17 rearrangements with respect of response to distinct therapies.

Abbreviations

ATCC: American Type Culture Collection; CEP17: chromosome 17 centromere; CGH: comparative genomic hybridization; Chr17: chromosome 17; ER: oestrogen receptor; PR: progesterone receptor; FISH: fluorescence *in situ* hybridization; IHC: immunohistochemistry; ISH: *in situ* hybridization; LOH: loss of heterozygosity; M-FISH: multi-color fluorescence *in situ* hybridization; SKY: spectral karyotyping; SRA: smallest region of amplification; TNBC: triple negative breast cancer.

Competing interests

The authors declare that they have no competing interests.

Authors' contributions

MRL performed G-Banding, karyotyping and M-FISH experiments, analyzed the data and participated to the manuscript writing; LVdC constructed the in house probe for STARD3, performed FISH experiments and analyzed the data; NR and SRRC participated to acquisition and analysis of G-Banding, karyotyping and M-FISH data; TM and GS participated to interpretation of FISH data and critically reviewed the manuscript; CM and AS conceived and designed the study, analyzed and interpreted the data and wrote the manuscript. All authors have given final approval of the manuscript.

Acknowledgements

This work was supported by AIRC (MFAG13310 to CM) and by Ricerca Sanitaria Finalizzata (RF-2010-2310674 to AS). Milena Rondón-Lagos is supported by the ERACOL program (Erasmus Mundus External Cooperation Window.EACEA/13/09 - Lot 21b).

Author details

[1]Department of Medical Sciences, University of Turin, Via Santena 7, 10126 Turin, Italy. [2]Department of Laboratory Medicine, Azienda Ospedaliera Città della Salute e della Scienza di Torino, Corso Bramante 88, 1026 Tutin, Italy. [3]Departments of Oncology and Clinical and Biological Sciences, University of Turin, San Luigi Hospital, Orbassano, Turin, Italy. [4]Natural and Mathematical Sciences Faculty, Universidad del Rosario, Bogotá, Colombia.

Received: 4 August 2014 Accepted: 27 November 2014
Published: 7 December 2014

References

1. Orsetti B, Nugoli M, Cervera N, Lasorsa L, Chuchana P, Ursule L, Nguyen C, Redon R, du Manoir S, Rodriguez C, Theillet C: **Genomic and expression profiling of chromosome 17 in breast cancer reveals complex patterns of alterations and novel candidate genes.** *Cancer Res* 2004, **64**(18):6453–6460.
2. Fraser JA, Reeves JR, Stanton PD, Black DM, Going JJ, Cooke TG, Bartlett JM: **A role for BRCA1 in sporadic breast cancer.** *Br J Cancer* 2003, **88**(8):1263–1270.
3. Greenberg RA: **Recognition of DNA double strand breaks by the BRCA1 tumor suppressor network.** *Chromosoma* 2008, **117**(4):305–317.
4. McClendon AK, Osheroff N: **DNA topoisomerase II, genotoxicity, and cancer.** *Mutat Res* 2007, **623**(1–2):83–97.
5. Olivier M, Petitjean A, Marcel V, Petre A, Mounawar M, Plymoth A, de Fromentel CC, Hainaut P: **Recent advances in p53 research: an interdisciplinary perspective.** *Cancer Gene Ther* 2009, **16**(1):1–12.
6. Pritchard KI, Shepherd LE, O'Malley FP, Andrulis IL, Tu D, Bramwell VH, Levine MN: **HER2 and responsiveness of breast cancer to adjuvant chemotherapy.** *N Engl J Med* 2006, **354**(20):2103–2111.
7. Zhang W, Yu Y: **The important molecular markers on chromosome 17 and their clinical impact in breast cancer.** *Int J Mol Sci* 2011, **12**(9):5672–5683.
8. Sapino A, Goia M, Recupero D, Marchio C: **Current challenges for HER2 testing in diagnostic pathology: state of the Art and controversial issues.** *Front Oncol* 2013, **3**:129.
9. Marchiò C, Lambros MB, Gugliotta P, Di Cantogno LV, Botta C, Pasini B, Tan DS, Mackay A, Fenwick K, Tamber N, Bussolati G, Ashworth A, Reis-Filho JS, Sapino A: **Does chromosome 17 centromere copy number predict polysomy in breast cancer? A fluorescence in situ hybridization and microarray-based CGH analysis.** *J Pathol* 2009, **219**(1):16–24.
10. Courjal F, Theillet C: **Comparative genomic hybridization analysis of breast tumors with predetermined profiles of DNA amplification.** *Cancer Res* 1997, **57**(19):4368–4377.
11. Forozan F, Mahlamaki EH, Monni O, Chen Y, Veldman R, Jiang Y, Gooden GC, Ethier SP, Kallioniemi A, Kallioniemi OP: **Comparative genomic hybridization analysis of 38 breast cancer cell lines: a basis for interpreting complementary DNA microarray data.** *Cancer Res* 2000, **60**(16):4519–4525.
12. Arriola E, Marchio C, Tan DS, Drury SC, Lambros MB, Natrajan R, Rodriguez-Pinilla SM, Mackay A, Tamber N, Fenwick K, Jones C, Dowsett M, Ashworth A, Reis-Filho JS: **Genomic analysis of the HER2/TOP2A amplicon in breast cancer and breast cancer cell lines.** *Lab Invest* 2008, **88**(5):491–503.
13. Kytola S, Rummukainen J, Nordgren A, Karhu R, Farnebo F, Isola J, Larsson C: **Chromosomal alterations in 15 breast cancer cell lines by comparative genomic hybridization and spectral karyotyping.** *Genes Chromosom Cancer* 2000, **28**(3):308–317.
14. Dieci MV, Barbieri E, Bettelli S, Piacentini F, Omarini C, Ficarra G, Balduzzi S, Dominici M, Conte P, Guarneri V: **Predictors of human epidermal growth factor receptor 2 fluorescence in-situ hybridisation amplification in immunohistochemistry score 2+ infiltrating breast cancer: a single institution analysis.** *J Clin Pathol* 2012, **65**(6):503–506.
15. Annaratone L, Marchiò C, Russo R, Ciardo L, Rondon-Lagos SM, Goia M, Scalzo MS, Bolla S, Castellano I, Verdun di Cantogno L, Bussolati G, Sapino A: **A collection of primary tissue cultures of tumors from vacuum packed and cooled surgical specimens: a feasibility study.** *PLoS One* 2013, **8**(9):e75193.
16. Rondón-Lagos M, Verdun Di Cantogno L, Marchiò C, Rangel N, Payan-Gomez C, Gugliotta P, Botta C, Bussolati G, Ramírez-Clavijo SR, Pasini B, Sapino A: **Differences and homologies of chromosomal alterations within and between breast cancer cell lines: a clustering analysis.** *Mol Cytogenet* 2014, **7**(1):8.
17. Nomenclature ISCoHC: *An International System for Human Cytogenetic Nomenclature.* Basel: Karger, S.B; 2013.

18. Lu YJ, Morris JS, Edwards PA, Shipley J: **Evaluation of 24-color multifluor-fluorescence in-situ hybridization (M-FISH) karyotyping by comparison with reverse chromosome painting of the human breast cancer cell line T-47D.** *Chromosom Res* 2000, **8**(2):127–132.
19. Wolff AC, Hammond ME, Hicks DG, Dowsett M, McShane LM, Allison KH, Allred DC, Bartlett JM, Bilous M, Fitzgibbons P, Hanna W, Jenkins RB, Mangu PB, Paik S, Perez EA, Press MF, Spears PA, Vance GH, Viale G, Hayes DF, American Society of Clinical Oncology; College of American Pathologists: **Recommendations for human epidermal growth factor receptor 2 testing in breast cancer: American society of clinical oncology/college of American pathologists clinical practice guideline update.** *J Clin Oncol* 2013, **31**(31):3997–4013.
20. Sapino A, Maletta F, Verdun di Cantogno L, Macrì L, Botta C, Gugliotta P, Scalzo MS, Annaratone L, Balmativola D, Pietribiasi F, Bernardi P, Arisio R, Viberti L, Guzzetti S, Orlassino R, Ercolani C, Mottolese M, Viale G, Marchiò C: **Gene status in HER2 equivocal breast carcinomas: impact of distinct recommendations and contribution of a polymerase chain reaction-based method.** *Oncologist* 2014, **19**(11):1118–1126.
21. Bhargava R, Dabbs DJ: **Interpretation of human epidermal growth factor receptor 2 (HER2) in situ hybridization assays using 2013 update of American society of clinical oncology/college of American pathologists HER2 guidelines.** *J Clin Oncol* 2014, **32**(17):1855.
22. Tibau A, López-Vilaró L, Pérez-Olabarria M, Vázquez T, Pons C, Gich I, Alonso C, Ojeda B, Ramón Y, Cajal T, Lerma E, Barnadas A, Escuin D: **Chromosome 17 centromere duplication and responsiveness to anthracycline-based neoadjuvant chemotherapy in breast cancer.** *Neoplasia* 2014, **16**(10):861–867.
23. McDermott M, Anderson L, Shields L, O'Brien N, Prendergast A, Kennedy S, Gallagher W, Zagozdzon R, Byrne A, Crown J, Slamon D, O'Donovan N: **Increased co-amplification of HER2 and STARD3 in a cell line model of acquired lapatinib resistance.** In *The 104th Annual Meeting of the American Association for Cancer Research: 2013.* Washington, DC: AACR; 2013.
24. Jarvinen TA, Tanner M, Barlund M, Borg A, Isola J: **Characterization of topoisomerase II alpha gene amplification and deletion in breast cancer.** *Genes Chromosom Cancer* 1999, **26**(2):142–150.
25. Jarvinen TA, Tanner M, Rantanen V, Barlund M, Borg A, Grenman S, Isola J: **Amplification and deletion of topoisomerase IIalpha associate with ErbB-2 amplification and affect sensitivity to topoisomerase II inhibitor doxorubicin in breast cancer.** *Am J Pathol* 2000, **156**(3):839–847.

doi:10.1186/1471-2407-14-922
Cite this article as: Rondón-Lagos *et al.*: Unraveling the chromosome 17 patterns of FISH in interphase nuclei: an in-depth analysis of the *HER2* amplicon and chromosome 17 centromere by karyotyping, FISH and M-FISH in breast cancer cells. *BMC Cancer* 2014 **14**:922.